

DISCRETE FRACTURE NETWORK MODELING
IN A CARBON DIOXIDE FLOODED HEAVY OIL RESERVOIR

A THESIS SUBMITTED TO
THE GRADUATE SCHOOL OF NATURAL AND APPLIED SCIENCES
OF
MIDDLE EAST TECHNICAL UNIVERSITY

BY

JAVID SHIRIYEV

IN PARTIAL FULFILLMENT OF THE REQUIREMENTS
FOR
THE DEGREE OF MASTER OF SCIENCE
IN
PETROLEUM AND NATURAL GAS ENGINEERING

JUNE 2014

Approval of the thesis:

**DISCRETE FRACTURE NETWORK MODELING IN A CARBON DIOXIDE
FLOODED HEAVY OIL RESERVOIR**

submitted by **JAVID SHIRIYEV** in partial fulfillment of the requirements for the degree of **Master of Science in Petroleum and Natural Gas Engineering Department, Middle East Technical University** by,

Prof. Dr. Canan Özgen

Dean, Graduate School of **Natural and Applied Sciences** _____

Prof. Dr. Mahmut Parlaktuna

Head of Department, **Petroleum and Natural Gas Engineering** _____

Prof. Dr. Serhat Akin

Supervisor, **Petroleum and Natural Gas Engineering Dept., METU** _____

Examining Committee Members:

Prof. Dr. Mahmut Parlaktuna

Petroleum and Natural Gas Engineering Dept., METU _____

Prof. Dr. Serhat Akin

Petroleum and Natural Gas Engineering Dept., METU _____

Prof. Dr. Nurkan Karahanoglu

Geological Engineering Dept., METU _____

Asst. Prof. İsmail Durgut

Petroleum and Natural Gas Engineering Dept., METU _____

Dr. Kubilay Kumsal

Consultant, Valeura Energy Inc. _____

Date: 05.06.2014

I hereby declare that all information in this document has been obtained and presented in accordance with academic rules and ethical conduct. I also declare that, as required by these rules and conduct, I have fully cited and referenced all material and results that are not original to this work.

Name, Last name: Javid Shiriyev

Signature:

ABSTRACT

DISCRETE FRACTURE NETWORK MODELING IN A CARBON DIOXIDE FLOODED HEAVY OIL RESERVOIR

Shirihev, Javid

M.S., Department of Petroleum and Natural Gas Engineering

Supervisor: Prof. Dr. Serhat Akin

June 2014, 67 pages

Fracture analysis is crucial because of their abundance in reservoirs and can have a strong effect on fluid flow patterns. Accordingly, Discrete Fracture Network (DFN) model is an efficient alternative approach to modeling fractured reservoirs and it is a special tool that considers fluid flow and transport processes in fractured rock masses through a system of connected fractures. Unlike Dual Porosity Model, where a continuum approach is applied, DFN uses detailed information about fracture and fracture connectivity from data sources like fracture logs and pressure transient data to create distinct fracture sets. In this study, a heavy oil reservoir going through CO₂ injection is modeled using DFN approach. It was used as a tool for upscaling geologic information about fractures to the dual-porosity fluid flow simulation. A DFN sector model was created by conditioning to fractures observed in a core scanner and are validated by well test analysis from the field. It has been observed that history matches obtained using a DFN sector model was better than those obtained without upscaled fracture information.

Keywords: Discrete Fracture Network Modeling, Natural Fractures, Carbonates

ÖZ

KARBON DİOKSİT BASILMIŞ AĞIR PETROL REZERVUARININ AYRIK ÇATLAK AĞI MODELİ

Şiriyev, Cavit

Yüksek Lisans, Petrol ve Doğal Gaz Mühendisliği Bölümü

Tez Yöneticisi: Prof. Dr. Serhat Akın

Haziran 2014, 67 sayfa

Rezervuarlardaki çatlak sayısı göz ardı edilemeyecek kadar fazla ve akışkanın akım yönünü belirlemeye güçlü bir etkiye sahip olduğu için rezervuar modellemede çatlak analizi önemli bir yer kaplamaktadır. Bu nedenle kullanılan Ayrık Çatlak Ağrı (AÇA) yöntemi çatlaklı rezervuar modellemesi için etkili bir alternatif yaklaşımdır ve akışkanın bitişik çatlaklar yoluyla kayacın içinden akmasını ve taşınmasını değerlendirmek için özel bir araçtır. Nesne sürekliliği kullanılan İkili Gözenek Modellemesi'den farklı olarak AÇA çatlak logları, basınç gibi verilerden çatlak ve çatlak bağlantısıyla ilgili detaylı bilgiyi kullanarak farklı çatlak setleri oluşturuyor. Bu çalışmada CO₂ basımdan geçen ağır petrol rezervuarı AÇA yaklaşımı kullanılarak modellenmiştir. Bu araç çatlaklarla ilgili olan jeolojik bilginin ikili gözenek modeline işlenmesi için kullanılmıştır. Karot tarayıcısında gözlemlenen çatlaklara bağlı olarak AÇA sektör modeli oluşturulmuş ve sahadan gelen kuyu testi analizleri ile onaylanmıştır. Sonuç olarak, AÇA sektör modeli kullanılarak elde edilen tarihsel çakıştırmanın çatlak bilgileri eklenmeyen modelin tarihsel çakıştırmasından daha iyi olduğu gözlemlenmiştir.

Anahtar Kelimeler: Ayrık Çatlak Ağrı Modellemesi, Doğal Çatlaklar, Karbonat

To My Family

ACKNOWLEDGEMENT

I would like to sincerely thank my advisor, Dr. Serhat Akin, for his guidance and comments throughout this study. His encouragement made my work more and more interesting. Without his support, this study would not have been accomplished. Additional thanks for opportunities provided during this graduate study period.

I also want to thank my classmates and assistant group of Petroleum and Natural Gas Engineering Department for their friendship and motivation.

Special thanks to my examining committee members for their review of my thesis and for comments they made on it. Finally, thanks to the head of department Dr. Mahmut Parlaktuna for providing reference to the scholarship.

TABLE OF CONTENTS

ABSTRACT	v
ÖZ	vi
ACKNOWLEDGMENTS	viii
TABLE OF CONTENTS	ix
LIST OF TABLES	xi
LIST OF FIGURES	xii
LIST OF SYMBOLS AND ABBREVIATIONS	xiv
CHAPTERS	
1. INTRODUCTION	1
2. LITERATURE REVIEW.....	5
2.1 Approaches for Reservoir Modeling	7
2.1.1 Equivalent Porous Media	7
2.1.2 Dual-Porosity Model.....	8
2.1.3 Dual-Permeability Model.....	10
2.1.4 Multiple Interacting Continuum Model	10
2.1.5 Vertical Refinement Model.....	11
2.2 Advantages of DFN Approach.....	12
2.3 Data Acquisition for DFN Application.....	13
2.4 Limitations of DFN Approach	14
2.5 Carbonate Reservoirs and Application of DFN	14
3. STATEMENT OF THE PROBLEM	17
4. METHOD OF STUDY	19
4.1 Fracture Network Model Generation	19
4.1.1 Conceptual Models.....	20
4.1.2 Distribution Types.....	21
4.1.2.1 Vector Distribution.....	21

4.1.2.2	Scalar Distribution.....	23
4.1.3	Cubic Law	26
4.1.4	Other Fracture Parameters.....	27
4.2	Dynamic Analysis	28
4.3	Fracture Upscaling	29
4.3.1	Concept of CMG Stars	30
5.	FIELD DATA ANALYSIS AND RESULTS.....	33
5.1	Motivation of the Field.....	34
5.2	Fracture Parameters.....	40
5.3	Well Test Simulation.....	43
5.4	Reservoir Model Generation	47
5.5	CMG Stars Output.....	53
6.	CONCLUSION AND RECOMMENDATION	61
	REFERENCES	63

LIST OF TABLES

TABLES

Table 5.1 Fluid, Matrix and Well Parameters	43
Table 5.2 Input Viscosity Data for Oil Phase	48
Table 5.3 Input Data for Fluid Component Properties of the Simulated Sector	48
Table 5.4 Input Constants for the Viscosity Calculating Equation	49

LIST OF FIGURES

FIGURES

Figure 2.1 Matrix-Fracture Orientation and Interaction for DPM	9
Figure 2.2 Matrix-Fracture Interaction for DK Model.....	10
Figure 2.3 Matrix-Fracture Interaction for MINC Model	11
Figure 2.4 Matrix-Fracture Interaction for VR Model	11
Figure 2.5 Fracture-Vug Model with a Probability factor of “f”	15
Figure 4.1 DFNM Application Scheme as a Step from Real Reservoir to DCM	19
Figure 4.2 Fisher Distribution	21
Figure 4.3 Bivariate Normal Distribution	22
Figure 4.4 PDF of Different Scalar Distribution Types	25
Figure 4.5 Fracture Model Assumption behind Cubic Law	27
Figure 4.6 Lagrange and Hermite Cubic Shape Functions Used in Galerkin FEM... ..	29
Figure 5.1 Early Time Well Test Analysis for Figuring Out Fracture Permeability .	34
Figure 5.2 Build-Up Period Pressure Plot for a Well from the Field.....	35
Figure 5.3 Pressure and Pressure Derivative Plot for a Well from the Field	35
Figure 5.4 Pressure vs. Time Interval to the Power of $\frac{1}{2}$ for the Fracture Analysis ..	36
Figure 5.5 Pressure vs. Time Interval to the Power of $\frac{1}{4}$ for the Fracture Analysis ..	36
Figure 5.6 Core Samples from the Well which Analyzed in a Core Scanner	37
Figure 5.7 Structural Map of the Studied Field and Wells.....	39
Figure 5.8 Grid Sector Selected for the Generation of DFNM with Constant Flux ..	39
Figure 5.9 Definition of Orientation Parameters.....	40
Figure 5.10 Aperture Values vs. Normalized Probability Values.....	41
Figure 5.11 Logarithm of Aperture Values vs. Normalized Probability Values.....	41
Figure 5.12 Fracture Aperture Distribution Derived from Core Scanner, Well-3	42
Figure 5.13 Well Test Pressure Plot vs. Time for Well-1	44
Figure 5.14 Well Test Pressure Derivative Plot of Build-up period for Well-1	44
Figure 5.15 Well Test Pressure Plot vs. Time for Well-2	45

Figure 5.16 Well Test Pressure Derivative Plot of Build-up period for Well-2	45
Figure 5.17 Well Test Pressure Plot vs. Time for Well-3.....	46
Figure 5.18 Well Test Pressure Derivative Plot of Build-up period for Well-3	46
Figure 5.19 Fracture Mesh Generated in FracMan after Dynamic Analysis	47
Figure 5.20 Input Oil/Water Relative Permeabilities for Liquid Phase, Matrix	49
Figure 5.21 Input Ternary Diagram of k_{ro} for Liquid and Gas Phase, Matrix	50
Figure 5.22 Input Oil/Water Relative Permeabilities for Liquid Phase, Fracture.....	50
Figure 5.23 Input Ternary Diagram of k_{ro} for Liquid and Gas Phase, Fracture.....	51
Figure 5.24 DFN Model Generated for Fracture Porosity	51
Figure 5.25 DFN Model Generated for Fracture Permeability in x direction.....	52
Figure 5.26 DFN Model Generated for Fracture Permeability in y direction.....	52
Figure 5.27 DFN Model Generated for Fracture Permeability in z direction	53
Figure 5.28 Oil Rate Match for Well-1	54
Figure 5.29 Oil Rate Match for Well-2	54
Figure 5.30 Oil Rate Match for Well-3	55
Figure 5.31 Water Cut Matches for the DFN and Conventional Models, Well-1	55
Figure 5.32 Water Cut Matches for the DFN and Conventional Models, Well-2	56
Figure 5.33 Water Cut Matches for the DFN and Conventional Models, Well-3	56
Figure 5.34 Oil Rate Extrapolation in DFN and Conventional Models, Well-3.....	57
Figure 5.35 Water Cut Extrapolation in DFN and Conventional Models, Well-3	58
Figure 5.36 Conventional Model, CO ₂ mole fraction at the end date, Layer 2	59
Figure 5.37 DFN Model, CO ₂ mole fraction at the end date, Layer 2	59
Figure 5.38 Conventional Model, CO ₂ mole fraction at the end date, Layer 3	60
Figure 5.39 DFN Model, CO ₂ mole fraction at the end date, Layer 3	60

LIST OF SYMBOLS AND ABBREVIATIONS

Symbols

$2b$	hydraulic aperture
avg	first correlation coefficient of viscosity and temperature, gas phase
bvg	second correlation coefficient of viscosity and temperature, gas phase
C	fluid compressibility
e	aperture
$f(x)$	density function
g	earth gravitational acceleration
k_n	normal stiffness
MW	molecular weight
N	number of gas components
N_f	number of hydraulically active fractures
S	storativity
T	transmissivity
y	gas mole fraction
$\Gamma(x)$	gamma function
μ	mean value
μ_a	absolute viscosity
ν	gas component viscosity
ρ	fluid density
σ	standard deviation

Abbreviations

BEM	Boundary Element Method
CMG	Computer Modeling Group
DCM	Dual-Continuum Model

DFN	Discrete Fracture Network
DFNM	Discrete Fracture Network Modeling
DK	Dual-Permeability
DP	Dual-Porosity
DPM	Dual-Porosity Model
EPM	Equivalent Porous Media
FEM	Finite Element Method
FINT	Fracture Intensity
MINC	Multiple Interacting Continua
PDF	Probabilistic Density Function
REV	Representative Elementary Volume
VR	Vertical Refinement

CHAPTER 1

INTRODUCTION

In all subsurface materials, discontinuities exist to some degree and occur on a scale ranging from micro cracks to crustal rifts. These discontinuities with the form of fractures in rock act as conductors providing preferential pathways for fluid flow with varying aperture, roughness, tortuosity and length that control the flow dynamics of fluid system. This conceptualization of fractured rock was first introduced by Snow (1965) who represented fracture networks with a series of interconnected parallel plates of variable aperture and length. The result is a highly heterogeneous and anisotropic model displaying hydraulic behavior that differs greatly from homogeneous models.

This conceptualization followed itself in Discrete Fracture Network (DFN) approach and since its introduction in the late 1970's, considerable controversy has aroused with fundamental concept of the Representative Elementary Volume (REV) which underpins all continuum approaches, Bear (1972). According to the REV concept, there exists a scale at which individual heterogeneities and discrete features can be ignored, due to a process of averaging to produce an effective continuum medium. On the other hand, DFN modeling is the recognition that at every scale, fluid transport in fractured rocks tends to be dominated by a limited number of discrete pathways formed by fractures and discrete features.

In overall, the DFN model represents the natural fracture system consisting of a group of planes. Early models of fracture network were systematic as a group of previously defined fractures. This fracture network model was simple in which fractures were fixed, splitting the space in equal cubes and because of its unsubstantial representation of fractures, stochastic models soon were proposed, Jambayev (2013).

In the stochastic models, fractures are considered planar, finite and disk shaped. The methodology for the modeling of a fracture network has been developed by many authors. One of such models is Baecher model in which finite-size fractures are disks with random diameters and orientations. These distributed disks of different shape, size and direction at different locations of formation is the simplest stochastic assumption and as a result, fractures intersect with each other. Later this methodology has been reviewed and extended by other researchers such as Dershowitz and Einstein (1988).

DFN approach of today is stochastic model of fracture architecting that incorporates statistical scaling rules derived from analysis of fracture length, height, spacing, orientation, and aperture. The goal of DFN modeling is to represent the important aspects of fractures within the mathematical framework of numerical simulation and engineering calculations. It is an important vehicle for the simulation of flow and solute transport in a fractured rock mass and has become powerful tool for fractured reservoir characterization.

Particularly, the DFN approach can be defined as “analysis and modeling which explicitly incorporates the geometry and properties of discrete features as a central component controlling flow and transport” and it has focused on identifying those individual discrete features which provide discrete connections where the flow being carried the most. Implementation area of this approach is quite broad and it has found many applications in mining, civil, environmental, reservoir engineering and other geoscience-geoengineering fields. More specifically, this technique has been applied in hydraulic fluid transport and carbon sequestration modeling other than fractured reservoir characterization, Jin et al. (2007).

All in all, DFN model enjoys wide applications for fluid flow problems of fractured rocks, perhaps mainly due to the fact that it is to date an irreplaceable tool for modeling fluid flow and transport phenomena at both the near-field and far-field scales. The near-field applicability is where the dominance of the fracture geometry at small and moderate scales makes the volume averaging principle used for continuum approximations unacceptable at such scales, and the far-field applicability is where equivalent continuum properties of large rock volumes need to be approximated through upscaling and homogenization processes using DFN models with increasing model sizes. In the latter, special care is necessary because explicit representations of large numbers of fractures may decrease efficiency of direct DFN models and the continuum model with equivalent properties may become more attractive, Lanru et al. (2007).

CHAPTER 2

LITERATURE REVIEW

The DFN flow modeling is the most recent method, which relies on three-dimensional spatial mapping of fracture planes to construct an interconnected network of fracture surfaces. It recognizes fractures as separate elements and able to provide numerical solutions for flow within fractures that incorporate the contribution of flow from the surrounding matrix. In overall, DFN analysis is fundamentally about the development of an appropriate model which considers the role of known and unknown discrete features including flow and transport, and also the flow barriers such as argillaceous layer.

Before going further details, it is important to understand several definitions related with the fractures. In the literature, it is often possible to come across terms such as, microfractures which refer to fissures and macrofractures which refer to just fractures. The difference between these two categories mainly concerns the dimensions of the fractures. Moreover, fracture systems and fracture network may originate some confusion. The fracture system is formed by all fractures having the same mutually parallel direction and is a subdomain of fracture network meaning that fracture network is the result of various fracture systems. Lastly, a fracture in which relative displacement has occurred can be defined as a fault, while a fracture in which no noticeable displacement has occurred can be defined as a joint, Van Golf-Racht (1982).

A DFN model typically combines deterministic and stochastic discrete fractures. The deterministic fractures or in other words measurable fractures are those directly imaged through seismic or intersected in wells and can be defined by width, length and orientation. All these parameters are necessary for generating fracture systems. Others, usually smaller-scale fractures may not have been detected through seismic; referring to non-measurable fractures, yet may be very important for reservoir performance. These fracture systems are generated stochastically. The geometrical and physical properties for these stochastic fractures are assigned through Monte Carlo sampling of relevant distributions, which may also be conditioned to both structural geology and depositional framework. When these two types of fracture systems combined resulting fracture network refers to DFN model.

Stochastic simulation of fracture systems is the geometric basis of the DFN approach and plays a crucial role in the performance and reliability of DFN models. The key process is to create probabilistic density functions (PDFs) of geometric parameters of fracture sets such as densities, locations, orientations and sizes, based on field mapping results using borehole logging, surface mapping, window mapping or geophysical techniques such as seismic wave, electric resistance or magnetic resonance imaging methods, Balzarini et al. (2001). The generation of the realizations of the fractures systems according to these PDFs and assumptions about fracture shape is then a straightforward inverse numerical process.

When it comes to shape, fractures are represented as circular, rectangular or polygonal discontinuities mostly for purpose of convenience since the real shape of sub-surface fractures cannot be fully known. However, one argument is that, for large-scale DFN models with a very high density of fractures, the effect of fracture shape on the final results may be much reduced or diminished. On the other hand, shapes of individual fractures may become important in affecting fracture system connectivity if the population of fractures is not so large. The issue of fracture shape is an unresolved one and will remain so for the foreseeable future, Lanru et al. (2007).

Physical properties such as transmissivity or storage, and geometrical properties such as size, elongation and orientation are assigned to each polygon based upon measured data or geologically conditioned statistical distributions derived from measured values. These fractures can be arbitrarily located within the rock matrix and have any desired distribution of aperture, density and orientation.

After generation and evaluation of these discrete features a mixed analytical-numerical technique is used to calculate flow through the network. The resulting DFN model is a more realistic depiction of fracture flow dynamics that offers a means of modeling the complex fracture/matrix interactions at small and large scales than any other known models and brief review of them are given below. The other superiorities are discussed in the second section of this chapter.

2.1 Approaches for Reservoir Modeling

In the literature, other than DFN, there are several approaches usually used to describe fluid flow in naturally fractured petroleum reservoirs. More conventional method for simulating fracture dominated reservoirs is to represent the rock as a dual-porosity continuum. In this approach, the matrix is represented as blocks or slabs and the fractures are mathematically represented as another continuum spatially coincident with the block faces. Model approaches other than Equivalent Porous Media are the modified form of dual-porosity continuum where modifications occur in matrix and its contribution to flow.

2.1.1 Equivalent Porous Media

Equivalent Porous Media (EPM) attempts to represent fractured rock reservoirs as single porosity model. These models work under the assumption that at a large scale, a network of fractures will distribute flow much like porous media. The rock matrix and fractures are treated as one entity and parameters such as conductivity and porosity are given bulk values and do not distinguish between the two flow-regimes. It requires only bulk estimates of hydraulic properties and thereby, avoids the problem of detailed characterization of the fractured geometry, Bairos (2012).

The fractured rock can be modeled as EPM when a small addition or subtraction to the test volume does not significantly change value of equivalent permeability; and when an equivalent permeability tensor exists which produces the correct fluid flux under an arbitrary hydraulic gradient direction, Long et al. (1982). Moreover, DFN can be used for the derivation of equivalent continuum flow and transport properties in the fractured reservoirs. However, depending on the case the most efficient implementation for the modeling of this type of reservoirs can be obtained when the hybrid of DFN and EPM models is used and this convergence between two methods can increase geological realism of solute transport conceptual model; three cases are shown below.

In many geological environments, heterogeneously connected karstic or fractured rocks occur within stratigraphic columns containing units best represented by continuum elements. *Layered DFN/EPM Models* meet this by incorporating both DFN and EPM elements. Secondly, EPM models have always been able to represent a limited number of faults and fractures explicitly using the same volumetric elements that are used to represent other geologic materials. Where these few discrete features carry the vast majority of flow and transport, these EPM models could be considered a fairly straightforward *DFN/EPM Model implementation*. The last one, *Nested EPM/DFN Model* combine the use of DFN elements in the locations where fracture geometry is of most concern, such as at intersections with boreholes and tunnels, with EPM elements at less sensitive locations, Dershowitz et al. (2004).

2.1.2 Dual-Porosity Model

Dual-Porosity model (DP) is more conventional model to describe behavior in fractured reservoirs. In this approach most of the fluid storage is provided by the porous matrix represented as an idealized system of identical rectangular blocks, whose porosity is much larger than the porosity of the fractures, and the fluid flow occurs only in highly permeable fractures, represented as orthogonally connected planes. In other words, there is no direct communication between inter-blocks; neighboring blocks are connected through fracture flow only. The fluid or heat inside

matrix can be transferred only to fracture. The properties of each matrix block are represented as a symmetrical tensor, and the properties are continuous throughout the entire block. Smaller fractures within each matrix block are coupled to the rock by means of sigma factor, or shape factor, which is the representative term of fracture-matrix transfer. Flow towards the borehole is considered to take place in the network, while the matrix continuously fed the system of fractures under the flow conditions specified, Figure 2.1.

This model can provide an accurate representation of flow dynamics in a fractured reservoir; however, it fails to characterize the geometry of the discrete fractures, solution features, and bedding that control flow pathway geometry and thus is incapable of modeling geometry-dependent fracture flow that occurs in reality. Moreover, since it is assumed that fracture and matrix within a grid block are at the same depth, it is not possible to simulate gravity drainage effects with this model. Finally, a quasi-steady state assumed inside each matrix element may lead to incorrect results in reservoirs with large matrix elements, particularly at the initial stages of reservoir depletion due to delayed matrix response.

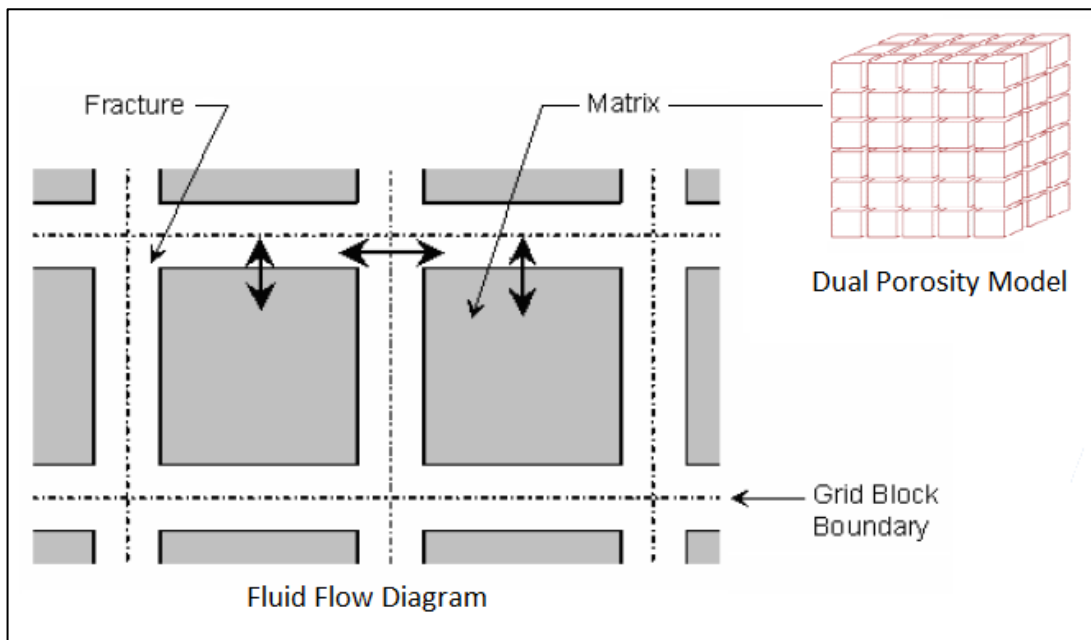


Figure 2.1 Matrix-Fracture Orientation and Interaction for DPM, STARS (2004)

2.1.3 Dual-Permeability Model

Dual-Permeability model (DK) is the other approach in which in comparison to the DP model, both the fracture network and the matrix participate in the fluid and heat flow. This model is suitable for moderately to poorly fractured reservoirs or fractured brecciated reservoirs where the assumption of complete matrix discontinuity is not valid. It is also used for problems which require capillary continuity. In comparison with dual-porosity model, gravity drainage can be simulated but only to a certain degree. This degree will vary with the complexity of a process and would be quite low for thermal heavy oil recovery, in which oil mobility is strongly temperature dependent. Furthermore, its computational demand is higher than any other methods.

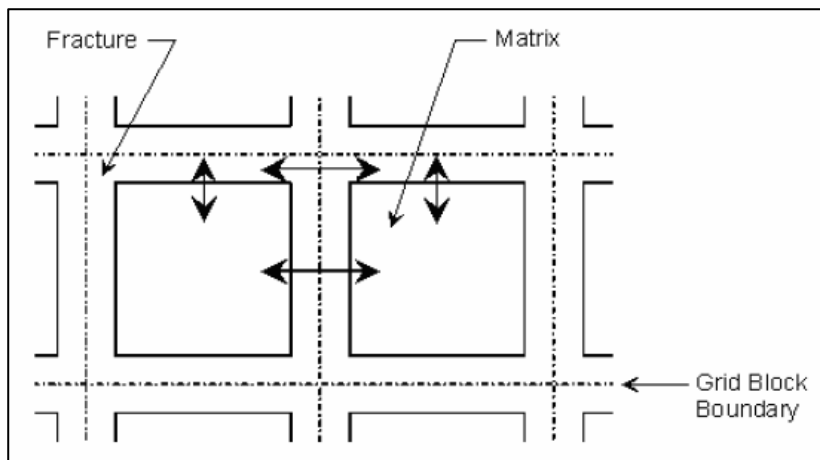


Figure 2.2 Matrix-Fracture Interaction for DK Model, STARS (2004)

2.1.4 Multiple Interacting Continuum Model

In MINC approach, matrix fracture interaction is efficiently modeled in terms of pressure transient within a matrix block. This matrix block is divided into several nested volume domains that communicate with each other. As a result, pressure, saturation, temperature gradients are established inside matrix, allowing transient interaction between two continua. Due to the matrix discretization, the transmissibility for matrix-fracture flow is higher than in DP or DK models for the same matrix size resulting in earlier and increased matrix-fracture response, Pruess et al. (1985).

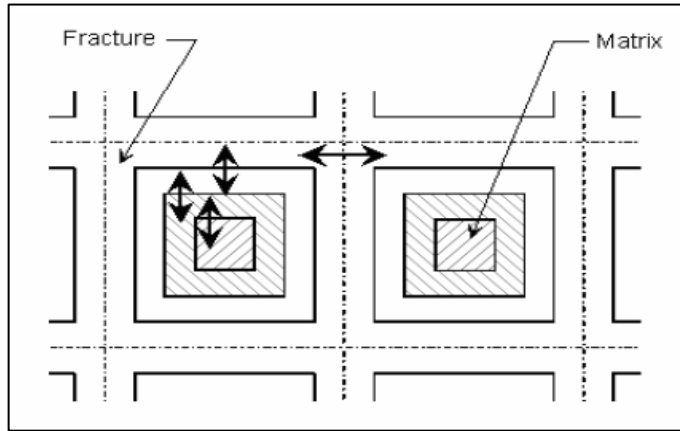


Figure 2.3 Matrix-Fracture Interaction for MINC Model, STARS (2004)

2.1.5 Vertical Refinement Model

VR model includes gravitational effects and considers gravity drainage mechanism. In this model matrix is refined in the vertical direction, accounting for transient flow behavior in the matrix, Figure 2.4. Complete phase segregation in the fracture is assumed. The sub-matrix blocks communicate with the fracture only in the horizontal directions, and with each other in vertical direction. These blocks have different depth and, hence, this model is suitable to simulate the gravity drainage process as well as processes with phase segregation inside the matrix. Similar to the MINC model, the fracture and matrix start communicating earlier due to smaller blocks.

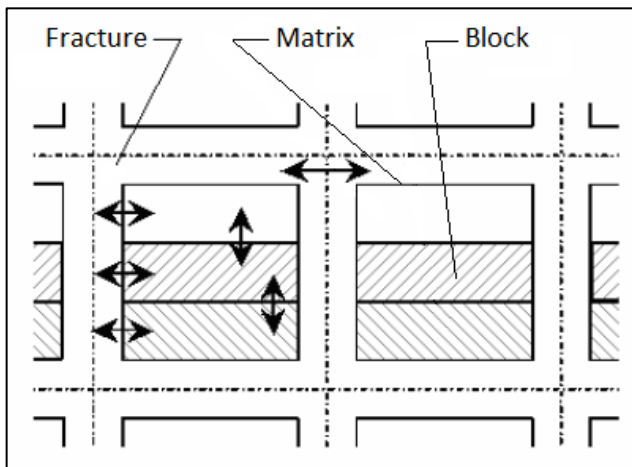


Figure 2.4 Matrix-Fracture Interaction for VR Model, STARS (2004)

2.2 Advantages of DFN Approach

The main advantage of a DFN model over above mentioned models is that fractures are represented as discrete features rather than being presented as a set of regularly spaced fracture network inside the matrix cubes. Particularly, DFN approach makes consistent use of a wide variety of disparate geological, geophysical and production data, which dual-continuum approaches cannot incorporate to the same extent.

The connectivity of a fracture system, which is a crucial topic for generating more reliable models, determines the fluid flow and transport processes in a fractured rock mass. The complexity of these flow systems makes it extremely difficult to characterize them with a great level of certainty on the field scale. Other than complexity of it, in many cases observed, only the small portions of the fracture population have been found to dominate the flow. Even domains that appear to be heavily fractured may not, in fact, be well connected. In a population of distributed fractures, the isolated fractures, which have no intersection with any other fracture, and singly connected fractures, which have only one intersection with other fractures, do not contribute to the flow field. In other words, fluid flow occurs through a series of connected fractures which transmits flow at a rate controlled by the properties of the fractures and the rock matrix.

In a DFN model this issue is handled more accurately than any other model. This approach more realistically models the connectivity of the faults and joints that give rise to reservoir-scale and well-scale non-continuum flow behavior. By using high quality of mapping techniques and then removing non-connected fractures the connectivity of the remaining fractures can be embedded to the model generated.

In overall, aforementioned EPM and dual-continuum modeling approaches cannot reproduce many commonly observed types of fractured reservoir behavior because they do not accurately reflect the geometry of fluid flow pathways. The inaccurate modeling of discrete feature connectivity results in inaccurate flow predictions in areas of the reservoir where there is not good well control.

2.3 Data Acquisition for DFN Application

Fracture parameters such as aperture, size, distribution and orientation are related to stresses, type of rock, structural conditions, depth, lithology, bed thickness and etc. Consequently, the variation in space of fracture characteristics are so irregular and complicated that the description of such a reservoir is substantially more difficult than that of a conventional reservoir, which makes the evaluation of fracturing far more complex than the evaluation of porosity and permeability in a conventional reservoir. Therefore, fracture detection and evaluation is based on the data gathered throughout all phases of reservoir development.

Fracture information is obtained during the exploration and production phases of field development and particularly in drilling, logging, coring and well testing. Observations on outcrops during the exploration phase, core examination in the laboratory, and the use of televiewer in the well during logging operations represent direct information. This type of evaluation on outcrops and on cores is mainly oriented towards the determination of the basic characteristics of fractures, such as width, orientation, length and etc. The indirect information is obtained during drilling, well testing and logging. In addition, the group of fractures is examined in order to evaluate their communicability, geometry and distribution, and eventually their intensity. According to Van Golf-Racht (1982), the best quantitative information concerning fracture parameters is obtained by direct measurement on outcrops and on cores obtained during drilling operations.

DFN approach also uses the same information sources for generation of the discrete fracture sets and in more detail, these sources involve lineament maps, outcrops, 2D and 3D seismic, well logs of various types, core, single well and multi-well production tests, flow logs, injectivity profiles, as well as structural or depositional conceptual models. Accordingly, specialized tools have been developed to derive the necessary input data for DFN models from these sources. For instance, packer testing is a conventional hydraulic testing technique often employed in the DFN approach to derive values of hydraulic conductivity and fracture aperture, Bairos (2012).

2.4 Limitations of DFN Approach

Although there are many benefits that DFN itself can bring in modeling of fractures, it may require detailed information and reliability of fractures will depend on the quality of the data. One of the two main input sources of DFN modeling is fracture system geometry which is based on stochastic simulations, using PDF of the geometric parameters of the fractures such as density, orientation, size, network information and etc. formulated according to field mapping results. However, region of direct mapping is limited and hence its adequacy and reliability is difficult to be evaluated.

Furthermore, fluid flux values in DFN numerical models are very sensitive to fracture aperture. Therefore, there is a great need to reduce errors in the characterization of fracture apertures as much as possible so as to ensure a high degree of accuracy in the output of these models. However, determination of aperture/transmissivity of fracture population, is also equally challenging, due to the fact that in situ and laboratory tests can only be performed with a limited number of fracture samples from restricted locations, and the effect of sample size is difficult to determine.

Finally, in reality, natural fractures in rock have tortuous geometries comprised of rough walls and varying apertures influenced by contact area of rock that often contribute to non-darcian flow dynamics. Nevertheless, many commercial codes developed for modeling fluid flow in fractured media including FracMan represent fractures as frictionless, parallel planes separated by a void space, Bairos (2012).

2.5 Carbonate Reservoirs and Application of DFN

All reservoirs are heterogeneous and naturally fractured to a certain degree where fracture refers to any break or crack including those cracks which can be identified by the presence of slickensides and mineralization, and these fractures are more common in carbonates than in sandstone. Moreover, approximately 60% of the world's oil is found in carbonate reservoirs which make characterization and modeling of it important.

Introduced DFN modeling approach has been used extensively for carbonate rocks for more than two decades, Dershowitz et al. (1988) and DFN modeling of carbonate rocks is significantly different from modeling for other geologies. While some fractured rocks can be treated as single porosity materials, carbonate rocks are frequently three porosity systems combining significant matrix permeability with fractures and solution features such as vugs and solution enhanced discrete pathways. Therefore, diverse procedures are required while applying DFN approach. These procedures provide a quantitative approach to description of the geometry and connectivity of solution features, fractures and bedding with their correlations. Hence, for more efficient work, while using DFN modeling in carbonate reservoir, following advanced approaches need to be considered.

Vugs are solution features which can range in size from millimeters to tens of meters. If a secondary vuggy type porosity has been developed in addition to intergranular porosity and if its volume is significant and uniformly distributed it needs to be taken account while modeling. Within DFN method, vugs can be generated as three-dimensional discrete features using either volume element or as a storage interaction term in the dual-porosity approach. Based on the contribution proportion, probability factors can be assigned to the vugs. In the Figure 2.5 basic two-dimensional idea of this scheme illustrated which was proposed by Erlich (1971) while studying relative permeability characteristics of vugular cores.

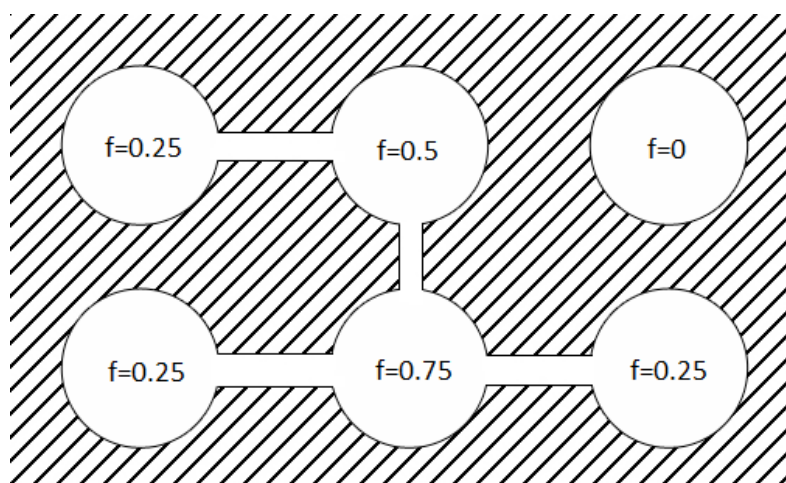


Figure 2.5 Fracture-Vug Model with a Probability Factor of “*f*”

Secondly, wormhole channels are solution enhanced fracture intersections which are major form of transport pathway in fractured carbonates. These channels frequently have apertures several times larger than those of the intersecting fractures. This can now be implemented in DFN models by adding pipe elements at karst enhanced fracture intersections. The extra storage and transmissivity of the wormhole channels can then be represented by a separate parameter.

Lastly, one of the key features of karstic carbonates is that certain portions of fracture planes have dramatically increased transmissivity and storage. This may be part of a continuous pathway (as in wormholes), or it may be a local effect. The karstic porosity on fracture planes can be modeled by tessellating the fracture surfaces, and applying the appropriate spatial pattern of karstic porosity to the planes, Dershowitz et al. (2004).

CHAPTER 3

STATEMENT OF THE PROBLEM

In conventional numerical reservoir simulation models, fractures are included as constant rock property which limits the output of the model to some extent. The primary aim of this study is to develop model which depicts fracture geology and includes heterogeneity of the physical properties of fractures more realistically. Geologic model of the fractures will be generated on the basis of observed static data and will be calibrated on the basis of flow data, well test matching. The mean of the immiscible CO₂ flow through realistically modelled reservoir, which is a function of fracture morphology indeed, is the other conclusion of this study.

CHAPTER 4

METHOD OF STUDY

In this chapter, stepwise procedure required for DFN approach is presented in detailed manner. After data analysis, generation of conceptual fracture network model is the initial step and theory behind is presented in the first section. Well test simulation is covered under the section of Dynamic Analysis. In the last section, process for the modeling of upscaled fracture is illustrated.

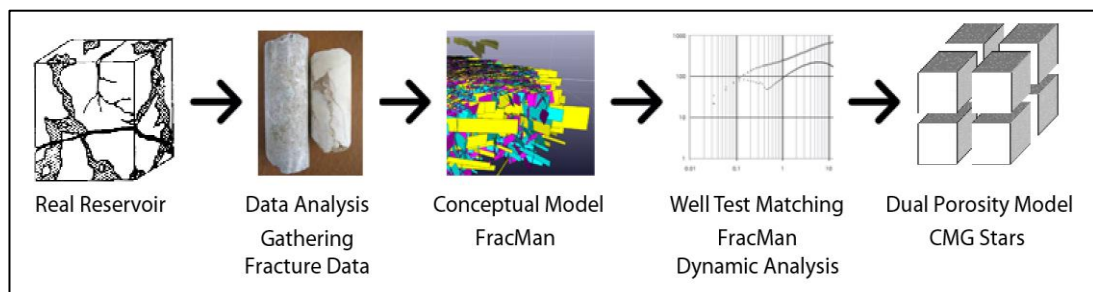


Figure 4.1 DFNM Application Scheme as a Step from Real Reservoir to DCM

4.1 Fracture Network Model Generation

Model generation region and algorithms for the fracture generation inside this region are the first step toward the conceptual model. There are six different types of fracture generation algorithms which use different stochastic processes yielding a distinct type of fracture set. The most basic one is the Geometric fracture set which uses surface regions as bounding layer and in this algorithm three different types of conceptual models can be used which is explained in 4.1.1 section. Geocellular type

of algorithm generates fractures inside the grid. Geologic fracture set is very similar to the Geocellular one, but it requires a Fold or Fault Model Grid to work. The other three generate fractures on the basis of tracemap, stress field properties and simulated geological unit.

4.1.1 Conceptual Models

There are three types of conceptual model algorithms for fracture generation used in FracMan software: Enhanced Baecher Model, Levy-Lee Fractal Model and Nearest Neighbor Model. These algorithms can be selected on the basis of what sort of behavior fractures are required to exhibit. They are demonstrated in a more detail below.

Enhanced Baecher Model: It is one of the first well characterized discrete fracture models and mainly generated by Poisson's process. This model is the extension of Baecher Model providing a provision for fracture terminations and more general fracture shapes. Initially discrete fractures can be generated as polygon structures with three to sixteen sides and then elongation parameters can be defined. In this model fractures are terminated at intersections with pre-existing fractures.

Levy-Lee Fractal Model: In general, fractal fracture patterns can be generated in three ways. Generation of fracture patterns in one scale and then superposition at different scales is one method. The other one is the generation of the fractures using non-fractal processes and then testing the resulting pattern whether it is fractal or not. Finally, fractures can also be generated on the basis of the Levy Flight process to produce clusters of smaller fractures around widely scattered larger fractures. This process refers to the algorithm used in FracMan and mathematically proven to produce fractal patterns.

Nearest Neighbor Model: This model is a simple, non-stationary model in which fracture intensity P32 decreases exponentially with distance from major features. P32 is the measurement of the fracture density by division of area of fractures to volume of rock mass ($A/V=1/L$).

4.1.2 Distribution Types

In FracMan, fractures are generated on the basis of several parameters which require distribution types and factors to be indicated. Generally, distribution types used are divided into two groups, vector and scalar distribution. A vector distribution involves parameters with multiple related parameters, such as orientation, which includes both a trend and plunge. This group uses distribution types from directional statistics subdivision of statistics. A scalar distribution creates a distribution of single values, for something such as fracture length which has only one value unrelated to other properties. The parameters which need to be specified with the distribution types are fracture orientation (vector distribution); fracture size (scalar distribution); fracture shape: aspect ratio (scalar distribution), elongation axis (vector distribution); and fracture aperture (scalar distribution).

4.1.2.1 Vector Distribution

Vector distribution types available in the software are Fisher, Bivariate Fisher, Bivariate Normal, Bingham and Bootstrap. Bootstrapping is also available for the scalar distribution but slightly different than with vector distribution.

Fisher or circular normal distribution shows an asymmetric property on the interval of $[0, \infty)$ and allows simpler statistical analysis compared to other circular distributions. As it is shown on the graph, every line with a different color represents different combinations of two degrees of freedom. As these degrees, numerator and denominator,

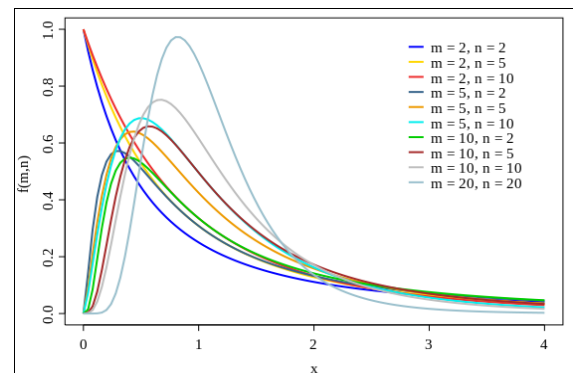


Figure 4.2 Fisher Distribution

increase dispersion of Fisher distribution decreases. In the software, indication of dispersion parameter is required after numerator, mean trend and denominator, mean plunge are specified. In some cases, Fisher distribution may not be satisfactory to

define orientation models, therefore, Bivariate Fisher distribution is presented and it is the generalization of Fisher distribution into two dimensions. In other words, it is spherical normal distribution. Therefore, after entering two mean trends and two mean plunges, two dispersion parameters are required for defining probability function in two-dimensional coordinate.

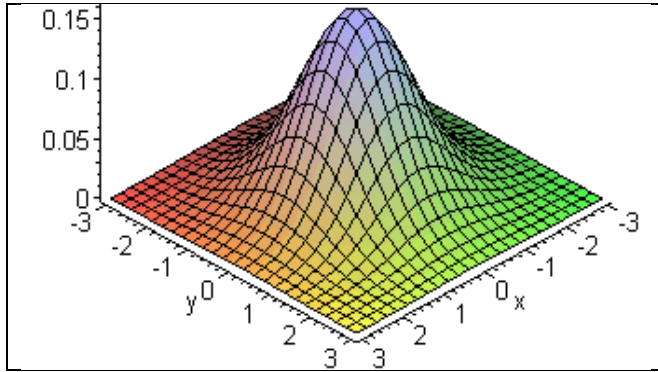


Figure 4.3 Bivariate Normal Distribution

The next one, Bivariate Normal distribution, is upscaling of normal distribution to two dimensions. To elaborate, if two parameters follow normal distribution separately, joint of the two linear combinations of these parameters will get Bivariate Normal distribution.

In the software, standard deviations of normally distributed pole trend and pole plunge and correlation coefficient between these parameters is required if this type of distribution is selected. The other one, Fisher-Bingham distribution is construction of the multivariate normal distribution on the surface of normalized sphere.

Fractured rock DFN models covering relatively large areas generally have a spatial variability in the fracture pattern. The orientation, size, and intensity of fracturing tend to vary across the site, such that statistically homogeneous models are inadequate. Bootstrap model starts with known values at specific locations and directly utilizes available data, rather than an interpolated field and it works well when there is good spatial coverage for data. In overall, bootstrap model looks for data which is relevant, and ranks that data by its relative relevance when generating a fracture at a specific location. Once a particular value is chosen, a small dispersion factor can be applied to account for the stochastic and spatial variability.

4.1.2.2 Scalar Distribution

Scalar distribution types available in the software are uniform, gamma, exponential, normal, log-normal, power law, weibull, poisson and constant values. In uniform distribution every value included in the continuous interval has the same probability of occurrence. The theoretical basis for the gamma distribution is the gamma function, a mathematical function defined in terms of an integral, Milton et al. (1995):

$$\Gamma(\alpha) = \int_0^{\infty} z^{\alpha-1} e^{-z} dz \quad \alpha > 0 \quad (4.1)$$

$$u > f(x) = \frac{1}{\Gamma(\alpha)\beta^\alpha} x^{\alpha-1} e^{-x/\beta} \quad x > 0; \alpha > 0; \beta > 0; \quad (4.2)$$

Gamma distribution gives rise to two families of random variables, one of which is exponential family. These variables are each gamma random variables with $\alpha=1$. The density for an exponential random variable therefore assumes the form:

$$f(x) = \frac{1}{\beta} e^{-x/\beta} \quad x > 0; \beta > 0; \quad (4.3)$$

The normal distribution is a distribution that underlies many of the statistical methods used in data analysis. It is often referred to as the “Gaussian” distribution. The density function of normal distribution is shown below, Milton et al. (1995):

$$f(x) = \frac{1}{\sqrt{2\pi}\sigma} e^{-(1/2)[(x-\mu)/\sigma]^2} \quad -\infty < x < \infty; -\infty < \mu < \infty; \sigma > 0; \quad (4.4)$$

Log-normal distribution is a continuous probability distribution of a random variable whose logarithm is normally distributed. A power law is a functional relationship between two quantities, where one quantity varies as a power of another.

$$f(x) = ax^k \quad (4.5)$$

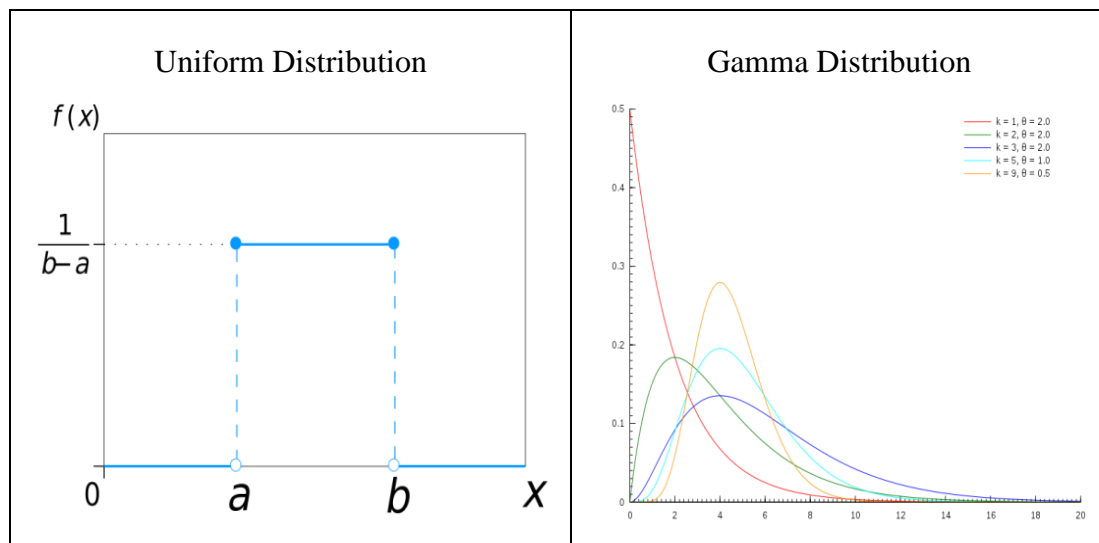
A random variable X is said to have a Weibull distribution with the scale parameter λ and shape parameter k ($\lambda > 0$ and $k > 0$) if the probability distribution function of X is:

$$f(x; \lambda, k) = \begin{cases} \frac{k}{\lambda} \left(\frac{x}{\lambda}\right)^{k-1} e^{-(x/\lambda)^k} & x \geq 0 \\ 0 & x < 0 \end{cases} \quad (4.6)$$

As the shape parameter k increases, density graph of Weibull distribution resembles that of the gamma density with the curve becoming more symmetric and exponential distribution is the special case of Weibull distribution with $k=1$. Lastly, Poisson distribution is a discrete probability distribution for the counts of events that occur randomly in a given interval of time or space with the density function given below:

$$f(x) = e^{-\lambda} \frac{\lambda^x}{x!} \quad x = 0, 1, 2, 3, \dots \quad (4.7)$$

In other words, Poisson processes involve observing discrete events in a continuous interval of time, length or space, for instance, number of fractures in a specified length. Lastly, constant value can be selected when the parameter is not available and iteratively changed for getting fractures verified. Graphs of scalar probability distribution function for all types are shown below:



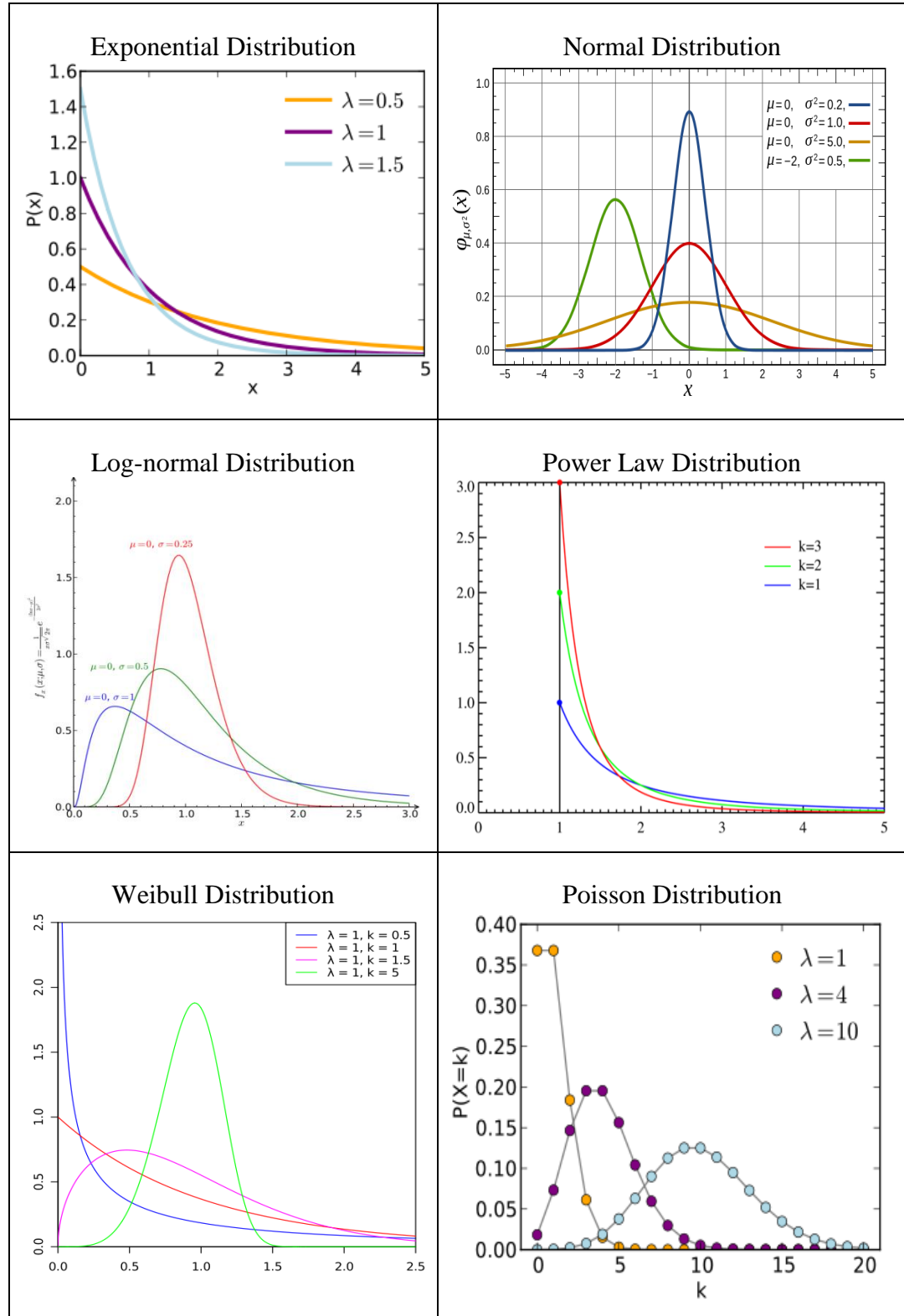


Figure 4.4 PDF of Different Scalar Distribution Types

4.1.3 Cubic Law

Fracture aperture with the other name fracture opening or fracture width shows the distance between the fracture walls in L dimensions and needs to be defined with a scalar distribution type. Moreover, it can be used in cubic law for drawing transmissivity input for fractures and there is an assumption made in this law which needs to be clarified. In reality, the fracture surfaces are rough and a repeatedly appearing finding is that fracture surfaces seem to exhibit fractal features. However, in the cubic law the rock fractures are most commonly assumed to be pairs of smooth and parallel planar surfaces separated by an aperture $2b$ as is shown in the Figure 4.5, Bairros (2012).

Flow takes place in between these two plates from inlet to outlet under a constant gradient bounded by rigid, impermeable walls that constitute no-slip boundary conditions at a specific width. In DFN models, this conceptual fracture model is applied to each individual fracture in a set to simulate flow. Such a simplification is particularly convenient for large-scale DFN models involving large numbers of fractures. This practice is based on the early work done by Snow (1965) and it is the simplest model of flow through a rock fracture and allows for simulations of dense, complex networks as they have a relatively low computational cost.

There is a challenging issue related with the definition of aperture which needs to be definite for evaluating transmissivity. Different definitions of fracture aperture exist in the literature: geometric aperture, mechanical aperture and hydraulic aperture. Transmissivity is a function of the hydraulic aperture and it is correlated with the cubic law equation as it is shown below:

$$2b = \sqrt[3]{\frac{12\mu_a T}{\rho g N}} \Rightarrow T = \frac{(2b)^3 \rho g N_f}{12\mu} \quad (4.8)$$

Where T symbolizes transmissivity, μ_a is absolute viscosity; ρ is fluid density, g is the earth gravitational acceleration, N_f is the number of hydraulically active fractures and $2b$ is the hydraulic aperture.

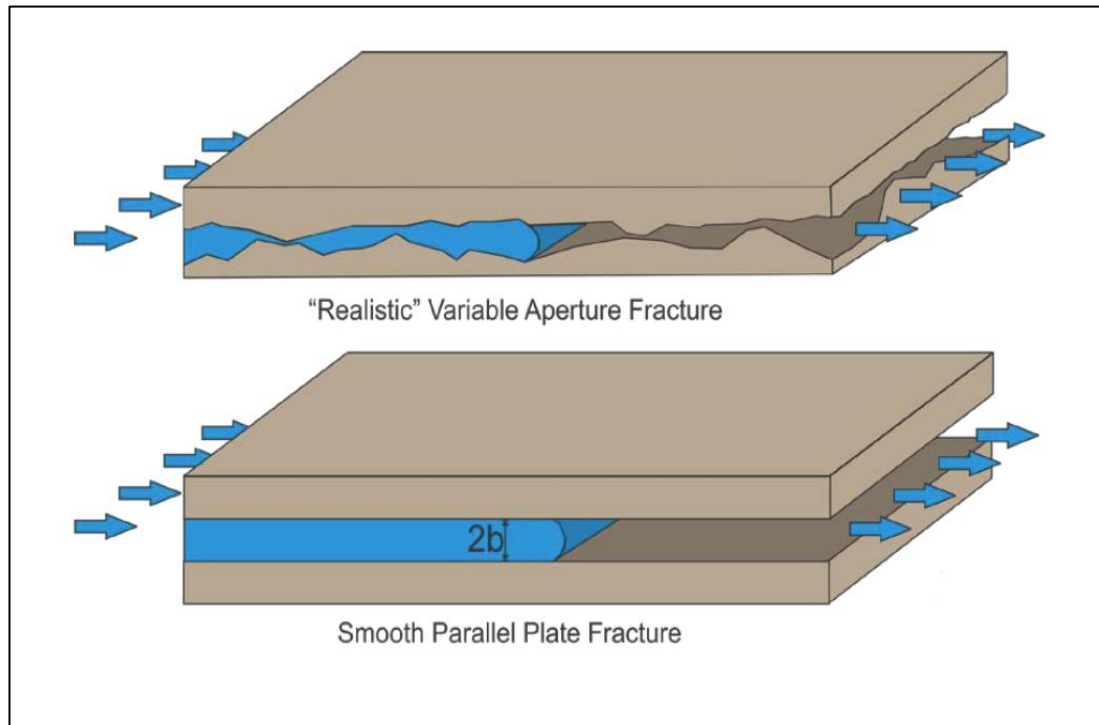


Figure 4.5 Fracture Model Assumption behind Cubic Law, Bairos (2012)

4.1.4 Other Fracture Parameters

There are several other parameters such as fracture storativity, intensity and shape (number of sides only) required to be defined, but not statistically before the generation of the fractures. Fracture storativity, as transmissivity, is correlated to fracture aperture. Equation below is used for the correlation based on the Doe et al. (1990):

$$S = \rho g \left(\frac{1}{k_n} + eC \right) \quad (4.9)$$

Where k_n symbolizes normal stiffness, e is aperture, C is fluid compressibility and S is the storativity. Fracture intensity, in the FracMan software, can be defined with P10, P32, P33 and fracture count where P10 is the number of fractures per length of scan line; P32 is area of fractures per volume of rock mass; and P33 is the volume of fractures per volume of rock mass. For defining fracture shape three parameters: number of sides, aspect ratio of elongation and elongation axis need to be defined.

4.2 Dynamic Analysis

After generating fractures and assigning physical properties, the next step is to simulate well test from dynamic analysis section. In the dynamic analyses of FracMan, fluid flow within fracture is assumed to obey to the Darcy flow equation where flow is taken parallel to the boundary surfaces of fractures. In the partial differential equation solved for the head, storativity, transmissivity and source term are involved. There are several numerical techniques developed for the solution of this PDE in individual fractures such as finite element method (FEM), boundary element method (BEM), simplified pipe networks and channel lattice models. The aperture of individual fractures is taken as a probabilistic distribution over individual fracture. In the FEM approach, because of this probabilistic distribution followed in aperture, its values vary element-by-element. The other approach, pipe network model represents the aperture field of a fracture by one or a set of connected pipes of effective hydraulic diameters according to the aperture values or distributions governed by results of measurements. Computational demand is much reduced when the pipe network models are used. However, FEM is one of the most famous methods in DFN flow models and is the one that is used in FracMan.

As a necessary part of FEM, in the generation of the finite element mesh number of nodes in the element can be deterministic in the accuracy of the solution and in time required for evaluation of the matrix. Too much nodes takes longer time for evaluating and not always is more precise than less number of nodes. Numbering the nodes is one another parameter for time efficiency of calculation. If the equation of the point under concern is dependent on the nodes those are closer to the node number of that point then less time is required for the matrix calculation. The other factor affecting duration of calculation is element side size; the less the size of element, the more elements, the much time it takes for calculation, however, the more accurate results we get. The mesh is automatically created in FracMan while well test simulation after the indication of maximum and minimum size of element. In general, the most primitive type of element is selected such as triangular in two dimensions.

Then, the shape functions are assigned to each node. There are several types of them used in FEM, such as Lagrange and Hermite cubic shape functions. Lagrange shape functions can take linear, quadratic and cubic forms. The shape function of specified node takes zero value in the other nodes and value of one only in its node. They show the weight factor of individual node on the point specified.

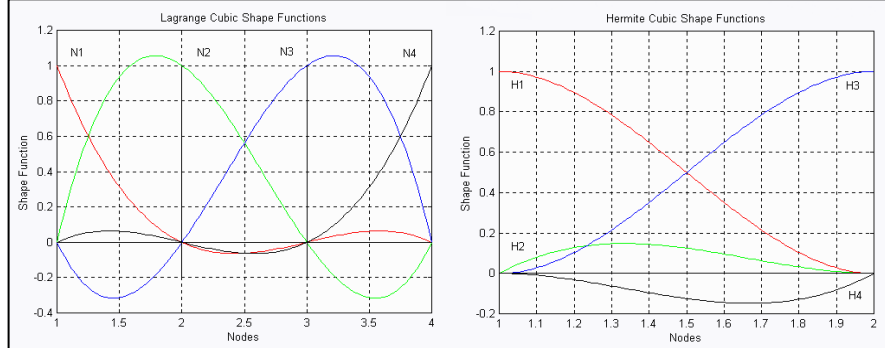


Figure 4.6 Lagrange and Hermite Cubic Shape Functions Used in Galerkin FEM

After generation of the mesh area, by applying Galerkin FEM method differential equation is converted to matrix form and then the solution of the matrix gives the nodal solutions which can be used to get values in the mesh area by summation of multiplications of nodal values with shape functions.

4.3 Fracture Upscaling

Afterward, equivalent grid cell permeability tensors need to be calculated as parameters to dual-continuum simulators. By applying unit pressure gradient in all three directions, computing the steady state flux across the cells of the grid and inverting Darcy's law for the flow, FracMan software generates permeability tensor for fracture flow. Resulting input data for CMG Stars contains information about the fracture permeability, porosity and shape factor for the fracture matrix interaction which is a function of fracture spacing. Warren and Root (1963) defined fracture shape as reflection of geometry of matrix elements and controlling factor between two porosity continuums. Gilman (2003) defined shape factor as a second order, distance related, geometric parameter used to estimate mass transfer from matrix to fracture.

4.3.1 Concept of CMG Stars

CMG STARS is a three-phase multi-component thermal and steam additive simulator. Grid systems generated for models may be Cartesian or cylindrical. Two-dimensional and three-dimensional configurations are available with any of these grid systems. The flow in naturally fractured reservoirs can be simulated by using four different models: dual-porosity, dual-permeability, multiple interacting continua (MINC) or vertical refinement (VR) depending on the process or mechanisms to be studied.

While DP selected, Warren and Root (1963) style dual-porosity option is used in the simulator; matrix and fracture systems can have its own porosity and permeability values, as well as other distinct properties. Inter-block flows are calculated in much the same manner as they would be in the standard model. These flows are governed by the fracture properties and an additional set of matrix-fracture flows is calculated. Thus, DP model allows one matrix porosity and one fracture porosity per grid block, where the matrix is connected only to the fracture in the same grid block. Fracture porosities are connected to other neighboring fracture porosities in the usual manner.

Input list of CMG STARS for model building requires nine different data groups (order is also important): Input-Output Control, Reservoir Description, Other Reservoir Properties, Component Properties, Rock-fluid Data, Initial Conditions, Numerical Methods Control, Geomechanical Model and Well & Recurrent Data. They are elaborated as in the following.

Input-Output Control define parameters that control the simulator's input and output activities such as filenames, units, titles, choices and frequency of writing to the output. Reservoir Description section contains data describing the basic reservoir definition and the simulation grid used to represent it. These data can be classified as: Simulation Grid and Grid Refinement Options, Choice of Natural Fracture Reservoir Options, Well Discretization Option, Basis Reservoir Rock Properties and Sector Options. Other Reservoir Properties contains data describing rock compressibility, reservoir rock thermal properties and overburden heat loss options. Component Properties indicate number of each type of component in preparation for fluid data

input. Rock-fluid Data define relative permeabilities, capillary pressures, component adsorption, diffusion and dispersion. In Initial Conditions section initial condition values of reservoir must present. Numerical Methods Control identifies the beginning of all numerical methods control keywords. In Geomechanical Model there are three separate model options: Plastic and Nonlinear Elastic Deformation Model, Parting or Dynamic Fracture Model and Single-Well Boundary Unloading Model; this is the only optional input data group. Well & Recurrent Data contains data and specifications which may vary with time. The largest part is well and related data, but there are keywords which define other time-dependent information also.

CHAPTER 5

FIELD DATA ANALYSIS AND RESULTS

Many classifications can be proposed for fractured reservoirs and one of them belongs to Nelson (2001). According to him, fractured reservoirs are categorized into four groups, based on porosity and permeability sharing between fracture and matrix. In the first type, both storage capacity and permeability comes from fracture. Second group includes reservoirs where matrix provides essential storativity and fractures provide essential permeability. Type three reservoirs involve fractures only for assisting matrix which has a good porosity and permeability value. In the last group, fractures have no significant role other than creating anisotropy.

In general, conventional approach for modeling fractured reservoirs is the dual-porosity model (DP) where reservoir rock is made up of two porosity systems; first one intergranular formed by void spaces between the grains of the rock, and a second formed by void spaces of fractures. However, combination of DFN and DP approaches is estimated to give the best solution. Rather than directly computing flow through a generated DFN using finite element simulations, dual-porosity parameters evaluated via Discrete Fracture Model for better production history matches. This approach is not new; history is older than a decade and has its own advantages such as decreasing time requirements for simulations.

In this contention, for analyzing DFN benefits on the CO₂ flooded heavy oil reservoir, segment of case field from Nelson second type category is handled with a limestone rock type. Moreover, reservoir has low pressure and low gravity oil, around 12 API. Viscosity of the oil is between 450 and 1000 cp and it contains low solution gas content. Average depth is 4300 ft. (1310 m) and gross thickness is 210 ft. (64 m). The reservoir rock exhibits heterogeneities in both horizontal and vertical directions. Average porosity is 18% and permeability taken from core samples is between 10 to 100 md. Analyzed well test data approve fracture existence by estimating effective permeability to be in the range of 200 to 500 md which is an indicator of dual-porosity system. Further analyses are carried out for understanding fractures in reservoir.

5.1 Motivation of the Field

Since well test data available from the field do not last long enough to see boundary effects, early time period analysis carried out for fracture study. This period of well test analysis can be indicative of fracture existence and its conductivity. If test data shows straight line behavior on the graph of square root of time interval vs. pressure difference, it means high permeability fractures are observed around the wellbore and if straight line fits to the graph of square root to the power of four, it concludes low permeability fractures, Figure 5.1, Horne (1990).

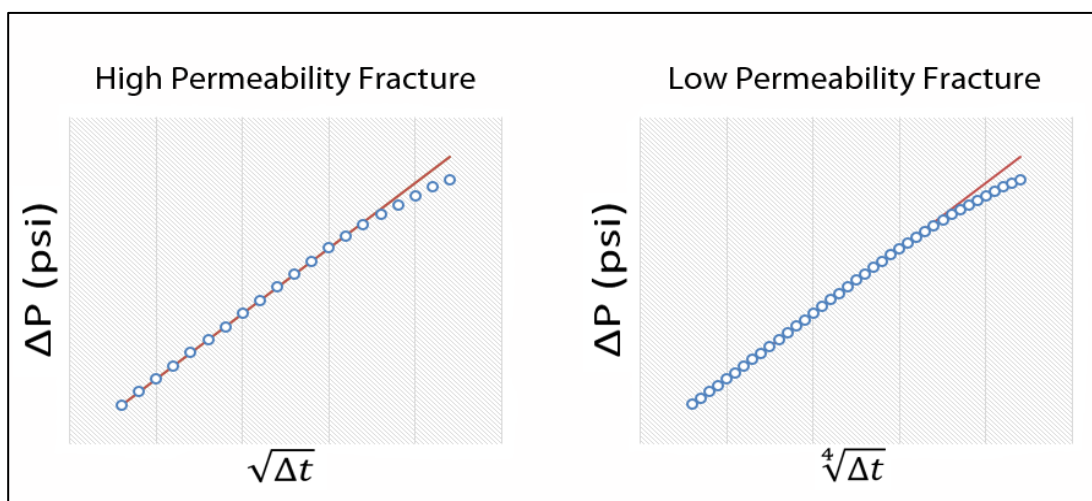


Figure 5.1 Early Time Well Test Analysis for Figuring Out Fracture Permeability

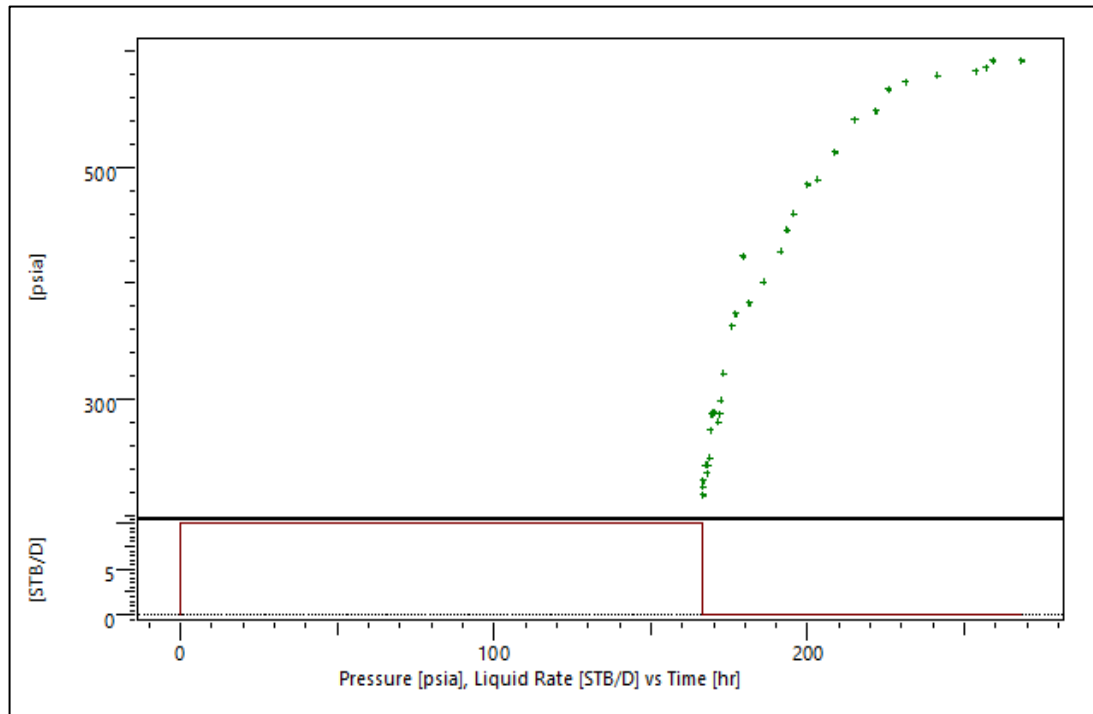


Figure 5.2 Build-Up Period Pressure Plot for a Well from the Field

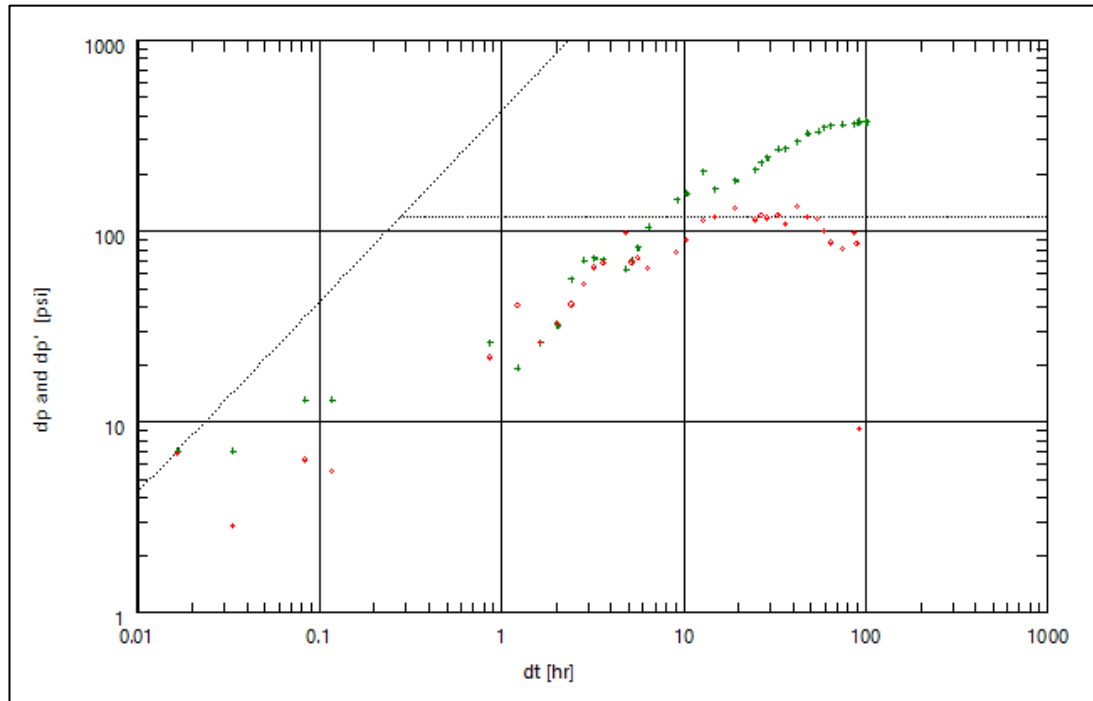


Figure 5.3 Pressure and Pressure Derivative Plot for a Well from the Field

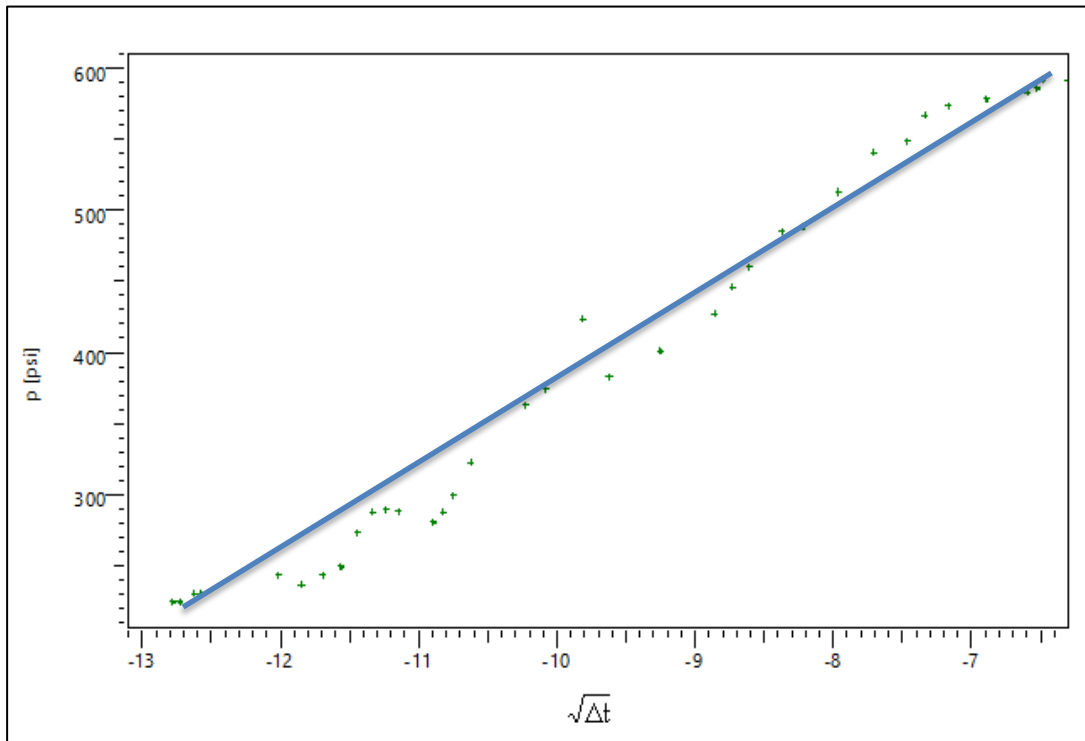


Figure 5.4 Pressure vs. Time Interval to the Power of $\frac{1}{2}$ for the Fracture Analysis

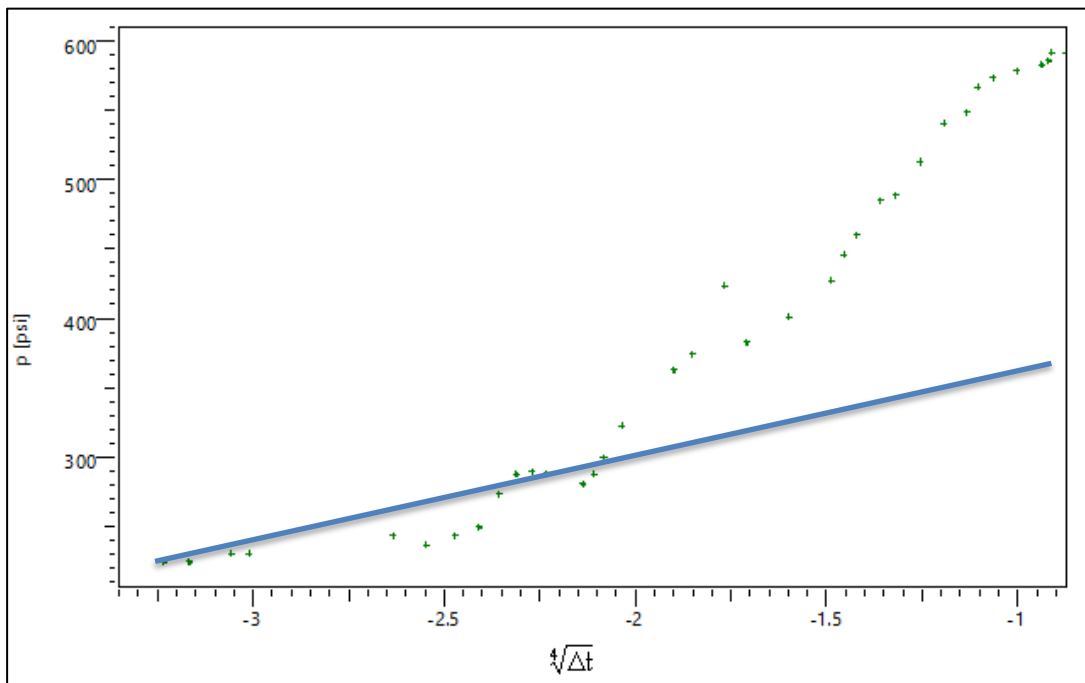


Figure 5.5 Pressure vs. Time Interval to the Power of $\frac{1}{4}$ for the Fracture Analysis

Well test analysis from one of the wells of the field is shown above. Build-up period of test from the Figure 5.2 is analyzed and derivative plot is shown on the Figure 5.3. In general, field is known to have high permeability fractures. As it can be seen from the Figures 5.4 and 5.5 better straight line match is obtained from the first case. Hence, well test data also conclude high permeability fractures around the wellbore.

Other than well test, the fracture aperture and intensity of core samples has been generated by digital core scanner, which takes 360 degree image of core samples and transmits it to the computer. The approach taken for vug and fissure characterization in the core samples was to run pixel count of the fissure from digital images. Core samples from one part of the well are shown on the Figure 5.6.



Figure 5.6 Core Samples from the Well which Analyzed in a Core Scanner

In comparison with fracture density in which degree of fracturing is defined through various relative ratios such as fracture bulk surface to matrix bulk volume, cumulative length of fractures to matrix bulk area in a cross flow section or number of fractures intersecting a straight line to the length of straight line, fracture intensity refers to ratio between fracture frequency and layer thickness frequency which is equal to FINT. If there exists only one layer of pay, the intensity is practically similar to the linear fracture density. Van Golf-Racht (1982) categorized degree of fracturing based on the value of FINT as below.

$FINT \geq 0.05$	Practically Fractured Zone	Category: 1
$FINT \approx 0.1$	Averaged Fractured Zone	2
$FINT = 5$ to 10	Strong Fractured Zone	3
$FINT = 20$ to 50	Very Strong Fractured Zone	4
$FINT \geq 100$	Breccia	5

In the studied case, this value for the core sample from the sector on average is equal to 31, Arslan et al. (2007), which belong to 4th category, very strong fractured zone. Hence, fracture intensity also concludes the same result as the well test analysis.

Lastly, in this field, it is believed that geometry and properties of discrete fractures play a significant role in the flow path and application of DFN approach seems to be reasonable and expected to give more accurate production history matches. Study is carried out to examine the convergence amount of the production history to the field data when DFN approach is used. With this intention, fracture network is generated and well test responses are simulated in FracMan software. Core scanner analyses as a scope of other study provide information about fracture aperture and intensity and are used in this stage. Well test responses from the field are used in dynamic analyses section for matching and validating fractures generated. Finally, upscaled geologic information is used in dual-porosity model which is simulated in CMG Stars software. This software also makes injection of CO₂ available which is required for figuring out difference of DFN outcomes over the conventional dual-porosity approach.

In the Figure 5.7, top view of the field is shown with the vertical well locations indicated. There are approximately three hundreds wells in the field, however, core scanner analysis are available only from few wells. Moreover, not all wells have well test analysis and not all of them are pretty satisfactory for reasonable conclusions. Therefore, a little sector is selected toward central west part of the field for the analysis. In this sector, core samples for Well-3 & their core scanner analysis and well tests are available from all of the three wells. Selected grid sector is shown in the Figure 5.8 with the conditioned well names, Well-1, Well-2 and Well-3.

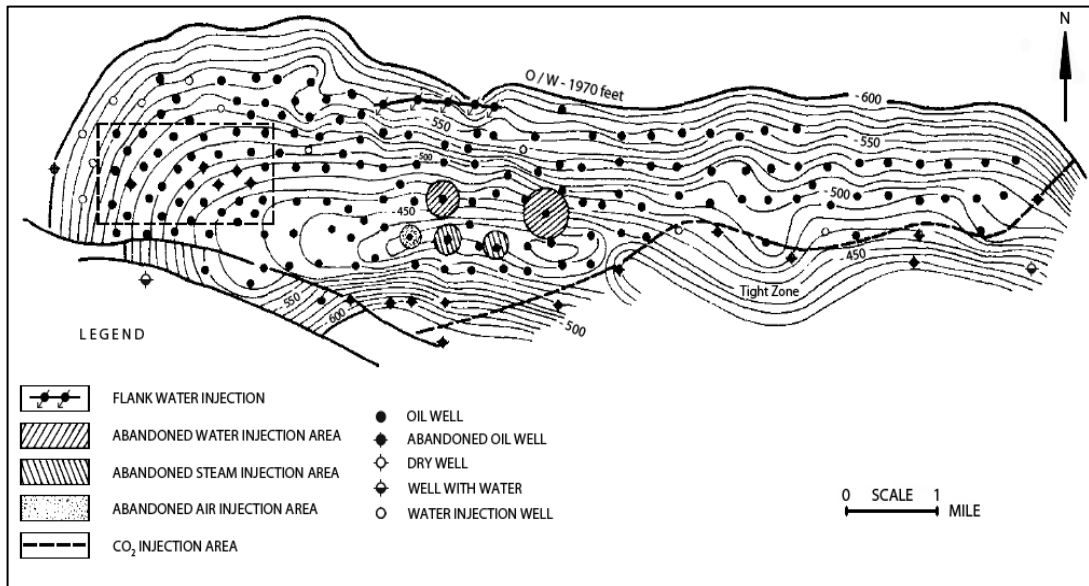


Figure 5.7 Structural Map of the Studied Field and Wells, Kantar et al. (1985)

All in all, core and well test analyses show major role of fractures in fluid flow pattern. In this field, CO₂ injection has been operated since 1980s and steam injection has been recently started. Therefore, for getting more converged model respond while reservoir evaluation, better characterization of the fractures becomes necessary part of a modeling.

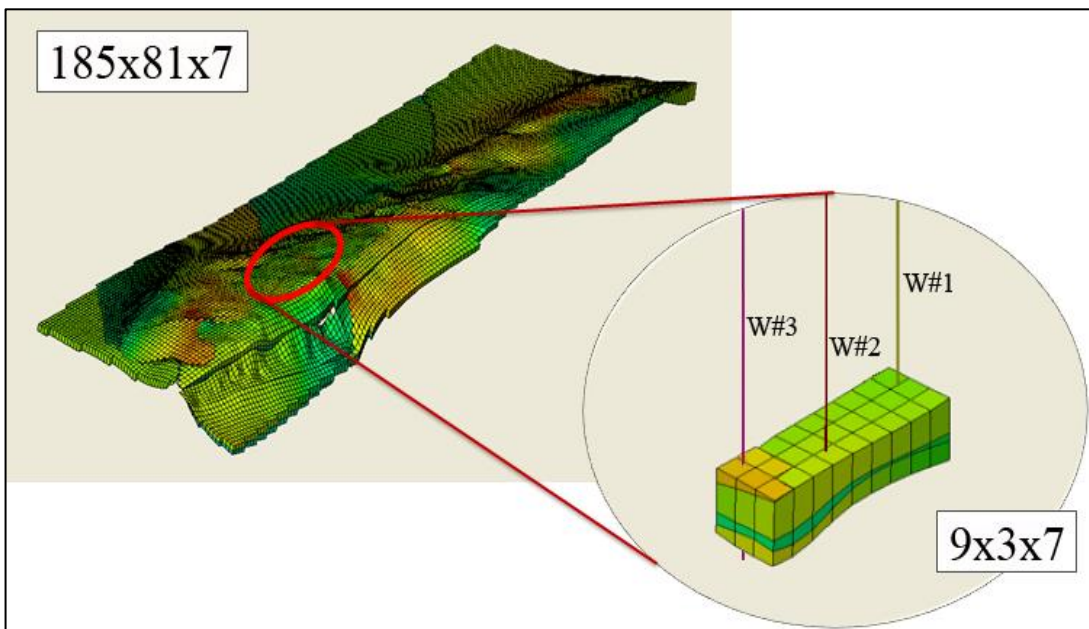


Figure 5.8 Grid Sector Selected for the Generation of DFNM with Constant Flux

5.2 Fracture Parameters

Core scanner analysis from Well-3 is used for the generation of deterministic fracture system by using Enhanced Baecher model. In this generated fracture system, only fracture shape is taken arbitrary because of the reason mentioned in Ch. 2. Since Levy-Lee Fractal Model can generate fractures locally, it is used for stochastic generation of fracture systems around Well-1 and Well-2. Resulting fracture network generated with geometric algorithm is the best model to get good well test matches on all of the wells.

For defining fracture orientation with the vector distribution two main parameters: dip angle and direction are crucial as it is shown on the figure. This information is obtained from previously handled study, Arslan et al. (2007). Based on

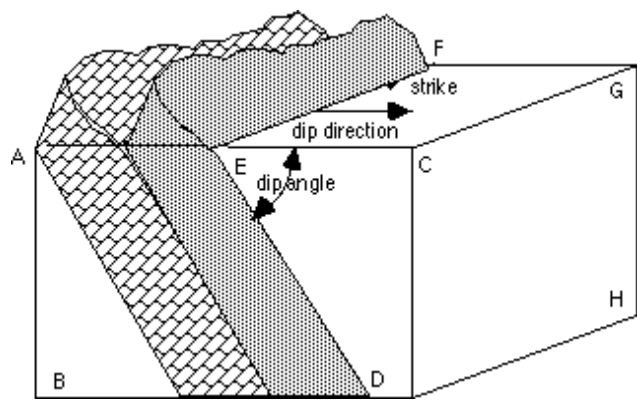


Figure 5.9 Definition of Orientation Parameters

this FMI log analyses, dip direction of the fractures for this sector region is taken to be N10E direction. Again from the same study fractures found to be mainly horizontally distributed. Deterministic fracture system generated in FracMan software will follow this trend. This is not necessary for the stochastically generated fracture systems, in general.

For aperture distribution input, core data is statistically analyzed to get distribution type, mean and variance. Normality check for the aperture values are handled by drawing normalized probability values vs. fracture aperture values in logarithmic and non-logarithmic forms. As it can be seen from the Figure 5.10 and Figure 5.11, since, better fit obtained to the straight line in logarithmic case, it can be concluded as log-normal distribution, Akin (2008). Histogram of these values also indicates log-normal distribution and it is shown on the Figure 5.12. Log-normal distribution with mean and variance values shown in this figure is selected for defining fracture apertures.

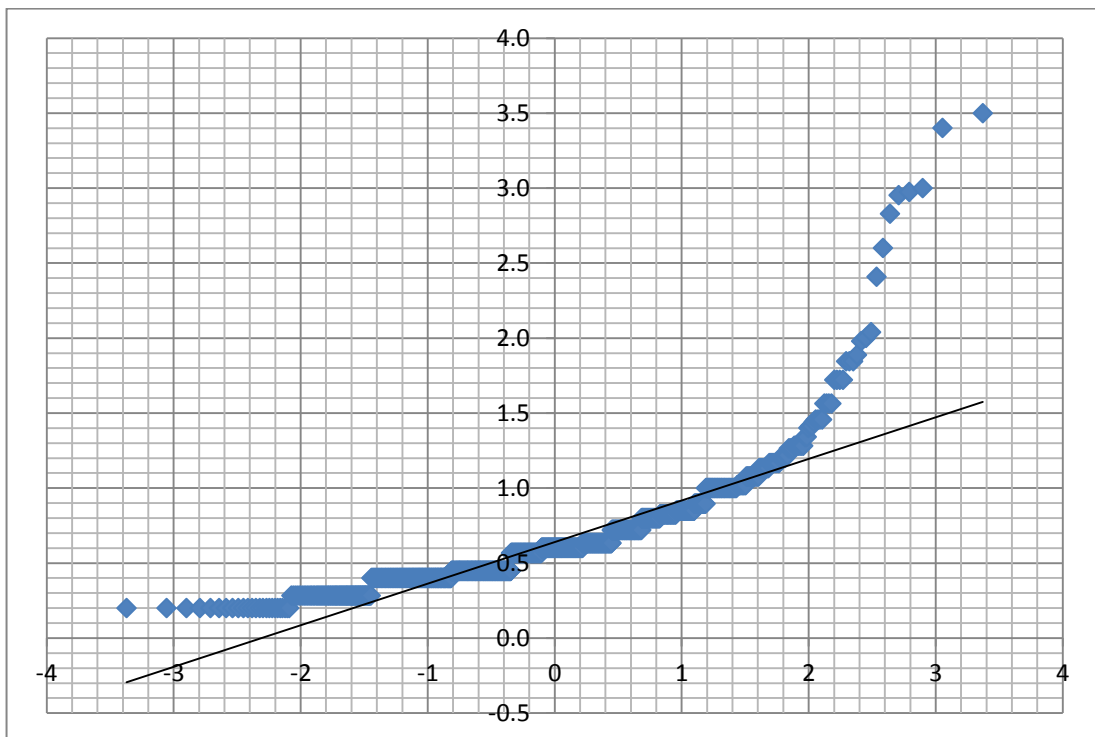


Figure 5.10 Aperture Values vs. Normalized Probability Values

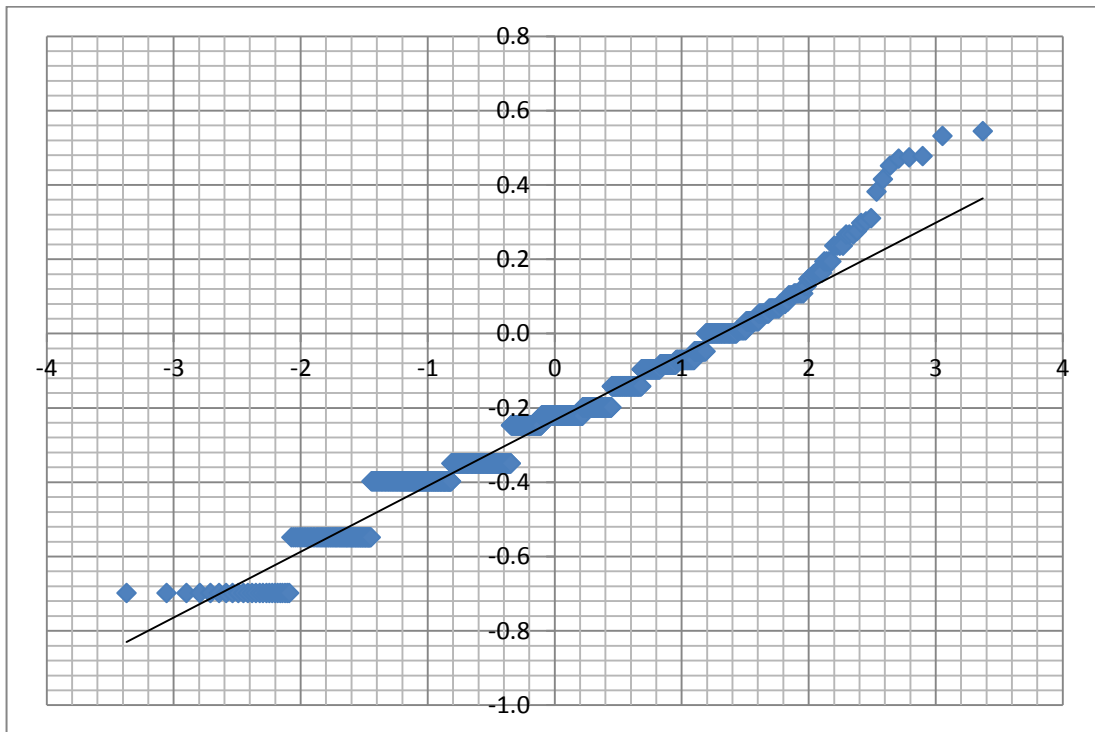


Figure 5.11 Logarithm of Aperture Values vs. Normalized Probability Values

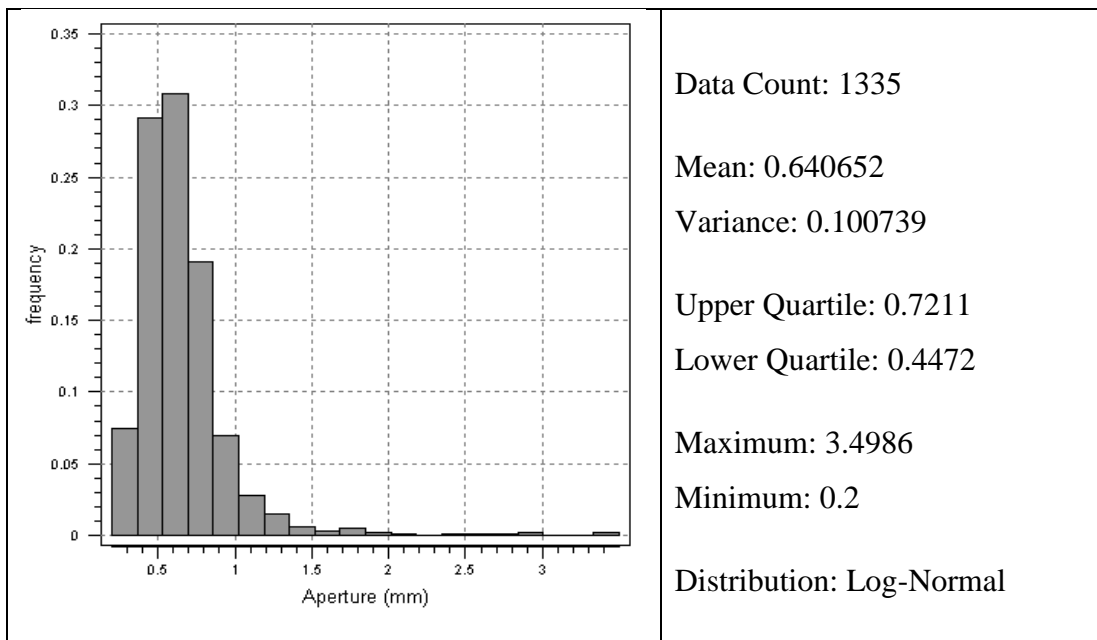


Figure 5.12 Fracture Aperture Distribution Derived from Core Scanner, Well-3

The other fracture parameter required for the generation of fracture system and defined with the scalar distribution type is fracture size, which refers to the relationship between fracture length and layer thickness; fractures can also be categorized on the basis of this parameter. Although there is no information about fracture size from the field, Van Golf-Racht (1982) proposed a direct relationship between fracture size and fracture aperture. Therefore, fracture size is assumed to be log-normally distributed because of the distribution type of fracture aperture. Arbitrary mean and variance values are taken on the basis of layer thickness.

While correlating transmissivity to the aperture with the Equation 4.8, N_f is taken equal to fracture intensity value which is available from the core scanner analysis. In the case studied, since intensity found in the core scanner analysis is in the form of number of fractures per length ($1/L$) it is defined with P10. For the last parameter, storativity aperture correlation Equation 4.9 requires normal stiffness for the fractures which is assumed to be 1000 GPa/m. Fluid PVT Data used for these two equations is shown on the Table 5.1 in the next section.

5.3 Well Test Simulation

Input data for FracMan Dynamic Analysis section are shown on the Table 5.1. This data includes fluid, well, matrix parameters and testing conditions. Depending on the model size mesh sizes can be increased to control simulation time. No major changes are made to deterministic properties; mainly parameters of stochastic fractures (fracture shape, size, orientation, apertures and others) are calibrated for obtaining better matches with the field well test data. The best matches obtained for the sector are shown on the Figures from 5.13 to 5.18. As it can be seen from the graphs, almost perfect match is obtained for the Well-3. Although well test data from the field for Well-1 and Well-2 are relatively poor compared to the Well-3, the matches obtained are fairly satisfactory when pressure drawdown is considered in pressure plot graphs. Fracture mesh generated while well test simulation is shown in the Figure 5.19.

Table 5.1: Fluid, Matrix and Well Parameters

FLUID PROPERTIES	Units	Well-1	Well-2	Well-3
Oil Density at 60°F	kg/m ³	983	984	991
Viscosity	cp	715	607	762
FVF	B/STB	1.0205	1.0205	1.0205
Compressibility	1/psi	8.61E-06	8.61E-06	8.61E-06
WELL PARAMETERS				
Storage	bbl/psi	1.25	0.876	0.209
Radius	ft	0.276042	0.276042	0.260417
Pay Zone	ft	75.4593	91.8635	157.48
Skin Effect	-	-2.18	20.5	-4.43
MATRIX PROPERTIES				
Permeability	md	10	10	20
Porosity	-	0.16	0.18	0.18
Compressibility	1/psi	3.00E-06	3.00E-06	3.00E-06
WELL TEST DATA				
Flow Rate	STB/d	31	30	150
Initial Pressure	psi	243.4	236.9	928
Duration of Test	hour	476	72	214.5

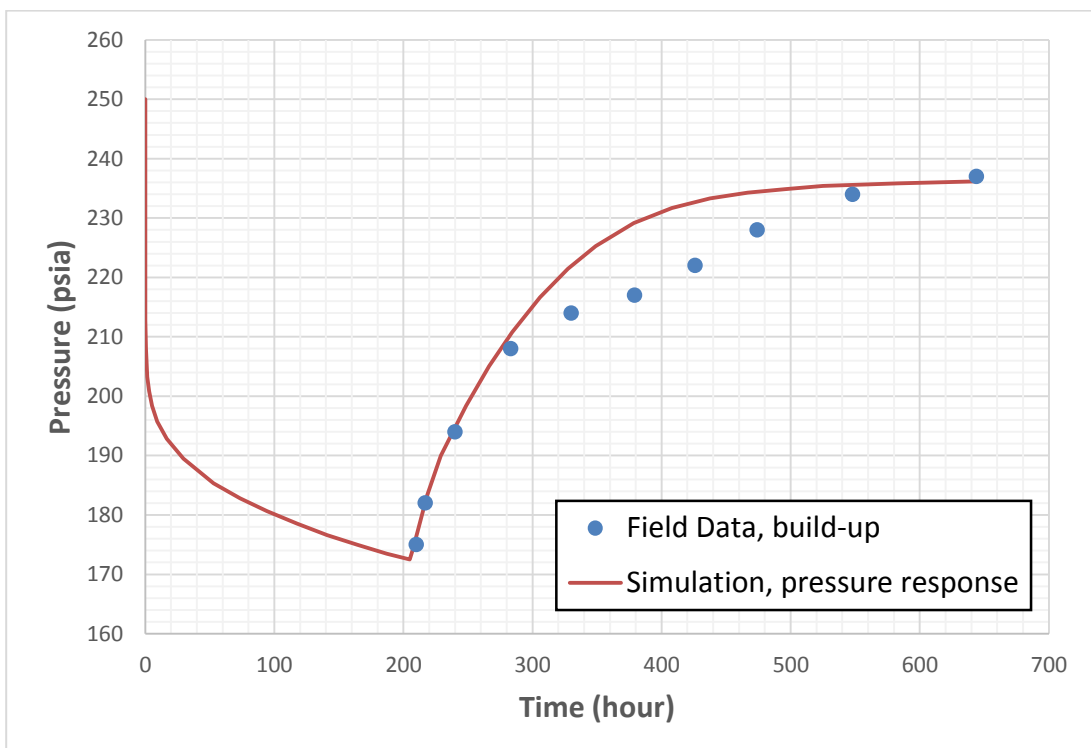


Figure 5.13 Well Test Pressure Plot vs. Time for Well-1

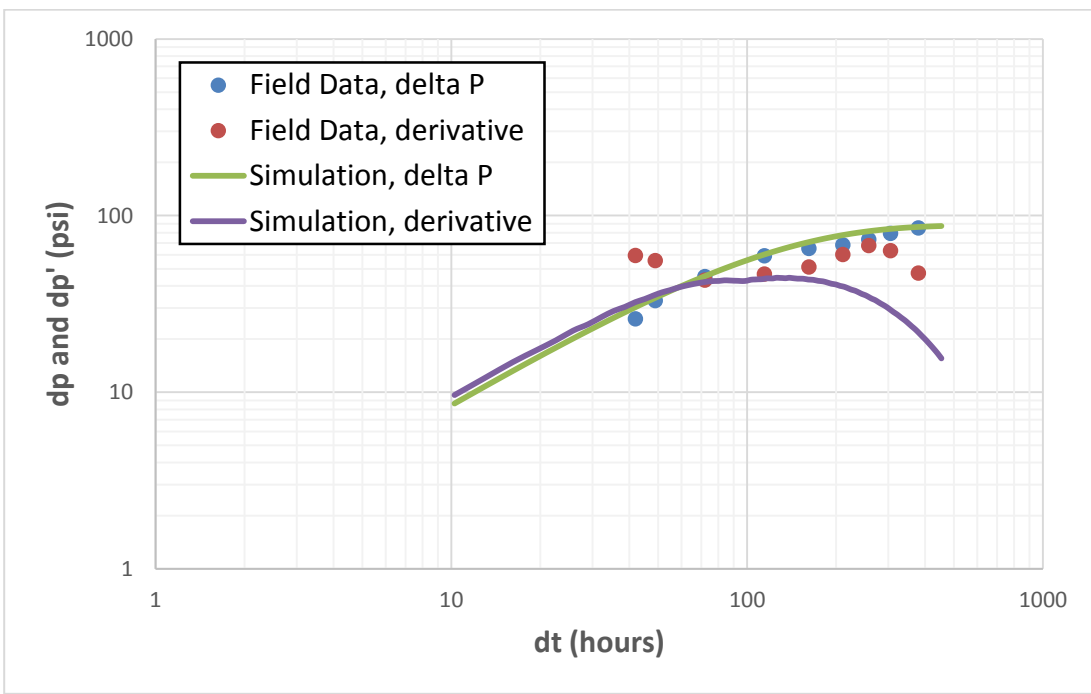


Figure 5.14 Well Test Pressure Derivative Plot of Build-up period for Well-1

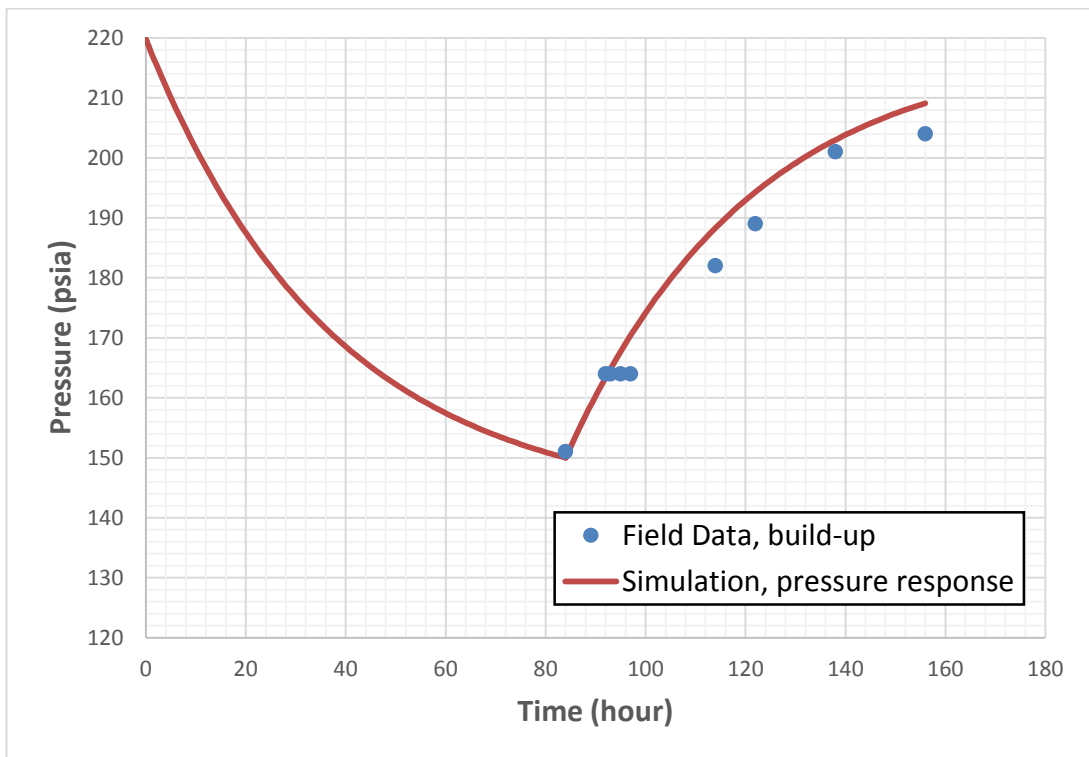


Figure 5.15 Well Test Pressure Plot vs. Time for Well-2

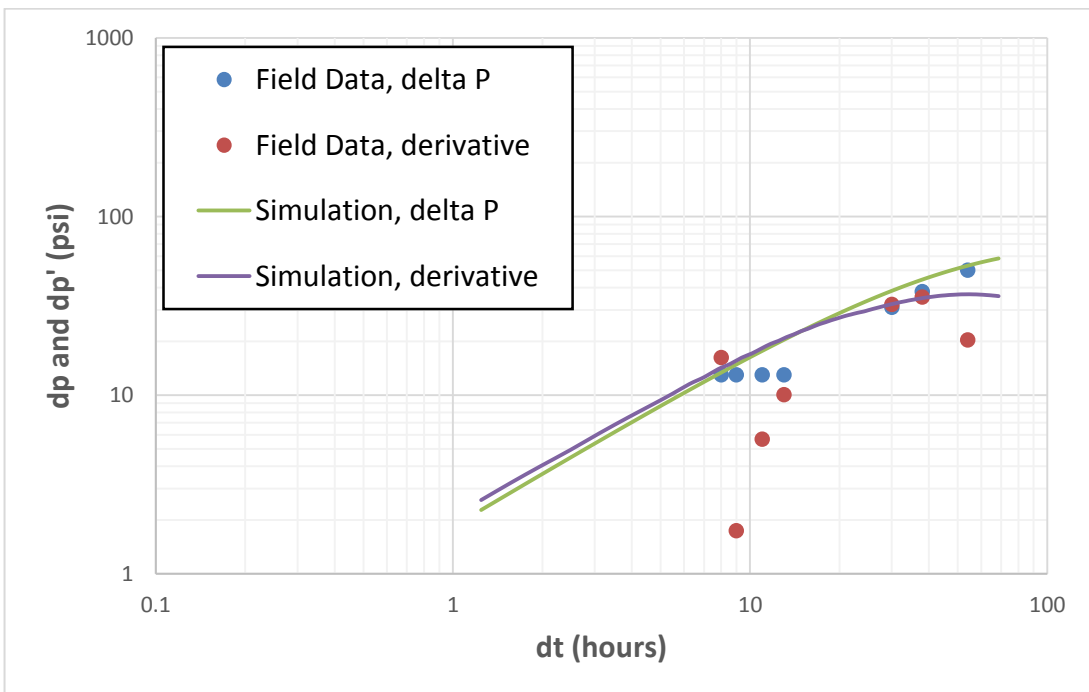


Figure 5.16 Well Test Pressure Derivative Plot of Build-up period for Well-2

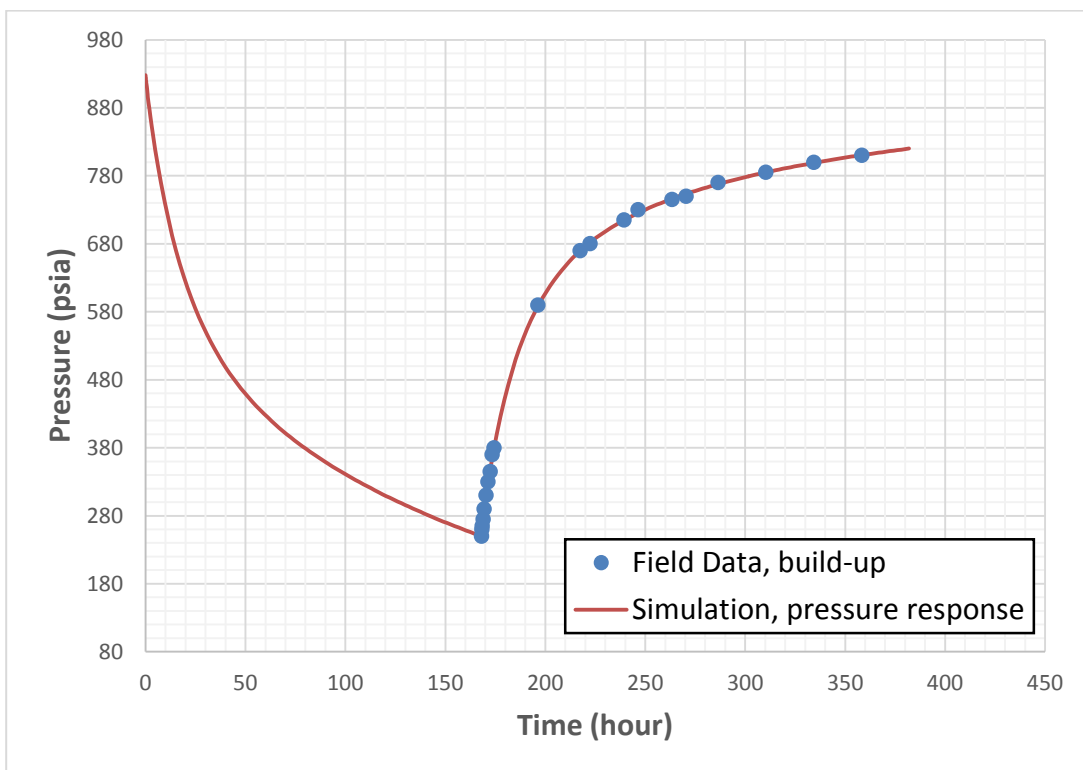


Figure 5.17 Well Test Pressure Plot vs. Time for Well-3

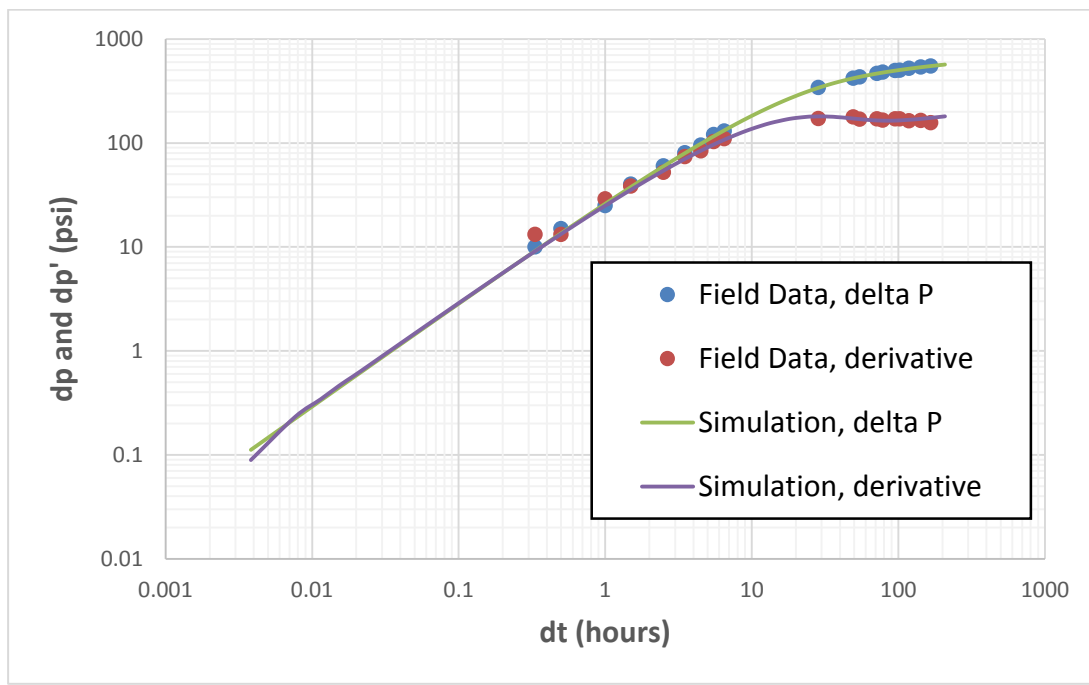


Figure 5.18 Well Test Pressure Derivative Plot of Build-up period for Well-3

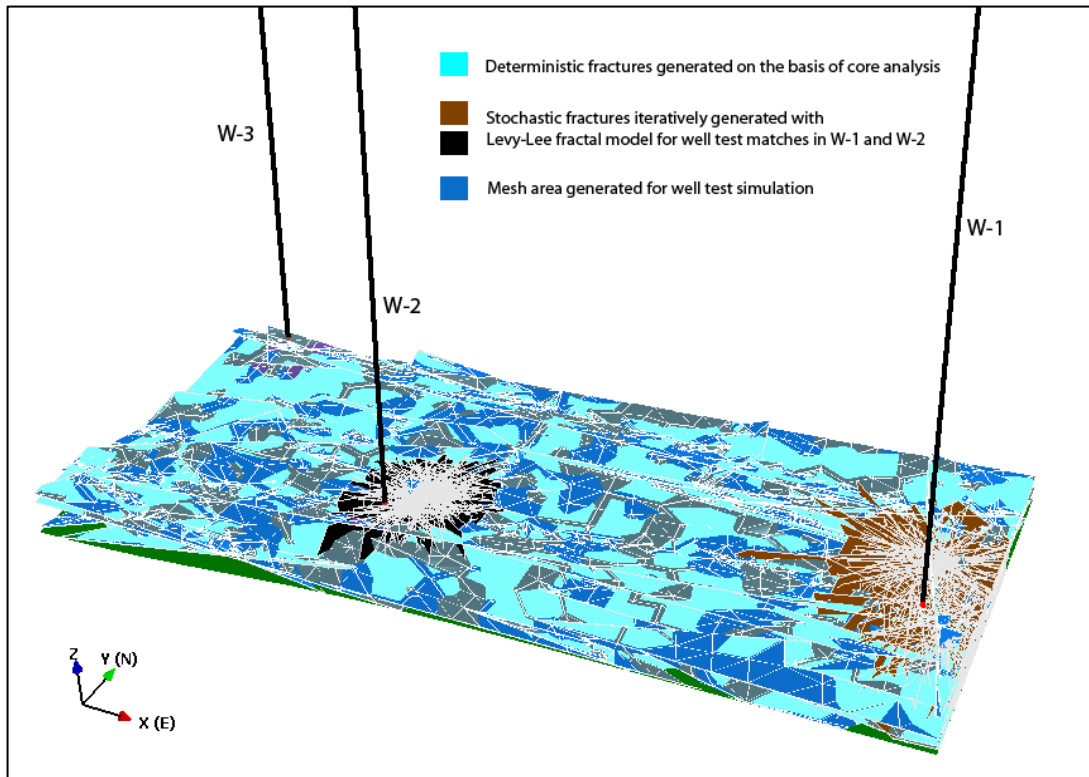


Figure 5.19 Fracture Mesh Generated in FracMan after Dynamic Analysis

5.4 Reservoir Model Generation

In the next step, permeability and porosity tensors for the grid cells are calculated in FracMan and exported to the CMG Stars simulation software where DP model is generated and executed for getting production history. After reservoir properties section of the input data which basically includes coordinates and properties of grids, component properties section proceeds where information about intensive and some extensive parameters of reservoir fluid is required. Study of these values is out of the scope of this thesis and is taken from the study of Akin et al. (2009). Petroleum is taken to include three types, light, medium and heavy oil with the initial proportions shown on Table 5.3. Two liquid phases, water and oil, are included in the production history match in the first period. In the final stage when CO₂ injection has started, gas phase is also included in the simulation. Although, temperature dependent viscosity for liquid phase is directly indicated in Table 5.2, for gas phase it is not the same.

Table 5.2 Input Viscosity Data for Oil Phase

Viscosity (cp)			
Temperature (°F)	Light Oil	Medium Oil	Heavy Oil
75	2.328	10.583	9109.65
100	1.9935	9.061	2370.22
150	1.4905	6.775	355.4
200	1.1403	5.183	92.46
250	0.8896	4.0434	32.5
300	0.7058	3.2082	13.8
350	0.5683	2.5833	6.76
500	0.319	1.4498	1.26
800	0.319	1.4498	0.14

In the CMG Stars, viscosity for gas phase while injection of CO₂ is calculated by the temperature dependent Equation 5.1, 5.2 and the avg and bvg values for the fluid phase is shown on the Table 5.4.

Table 5.3 Input Data for Fluid Component Properties of the Simulated Sector

	Water	Light Oil	Medium Oil	Heavy Oil	CO ₂
Molecular Weight (lb/lbmol)	18.02	250	450	600	44
Critical Pressure (psi)	3206.2	225	140	Non Volatile (0)	1029
Critical Temperature (°F)	705.4	800	950	Non Volatile (0)	88.7
Molar Density (lbmol/ft ³)	0	0.2092	0.1281	0.102	-
Liquid Compressibility at constant T (1/psi)	0	5.00E-06	5.00E-06	5.00E-06	-
Thermal Expansion Coefficient (1/°F)	0	3.80E-04	3.80E-04	3.80E-04	-
Liquid Enthalpy (BTU/lbmol)	0	132.5	247.5	360	-
Specific Heat Capacity (Btu/lb-°F)	-	0.53	0.55	0.6	-
Initial Phase Mole Fraction for Matrix	-	0.015	0.05	0.935	-
Initial Phase Mole Fraction for Fracture	-	0.015	0.05	0.935	-

$$\text{gas component viscosity} = \nu(i) = \text{avg}(i) \cdot T^{\text{bvg}(i)} \quad (5.1)$$

$$\text{overall gas phase viscosity} = \frac{\sum_{i=1}^N \nu(i) \cdot y(i) \cdot \sqrt{MW(i)}}{\sum_{i=1}^N y(i) \cdot \sqrt{MW(i)}} \quad (5.2)$$

Where y is the gas mole fraction of the component, MW is molecular weight, N is the number of gas components, and avg & bvg are the first and second correlation coefficient of viscosity and temperature, respectively.

Table 5.4 Input Constants for the Viscosity Calculating Equation for Gas Phase

	Water	Light Oil	Medium Oil	Heavy Oil	CO ₂
avg	1.13E-05	5.00E-05	1.00E-04	0	0.00107
bvg	1.075	0.9	0.9	0	0.8655

In the CMG Stars, fracture and matrix are taken to be two different rock types and relative permeability values need to be assigned for both of these types. Input curves for both one phase (liquid) and two phase (liquid and gas) period are illustrated on the Figures 5.20-5.23.

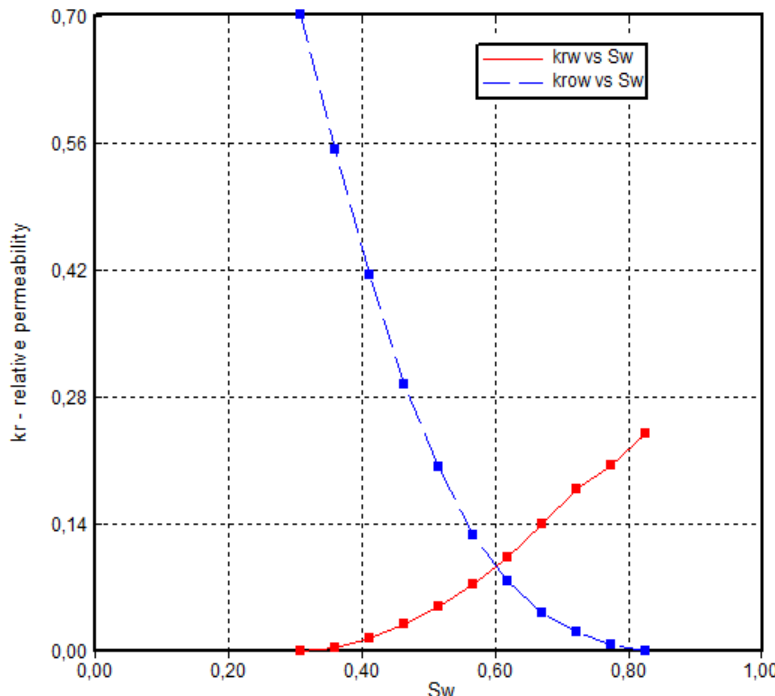


Figure 5.20 Input Oil/Water Relative Permeabilities for Liquid Phase, Matrix

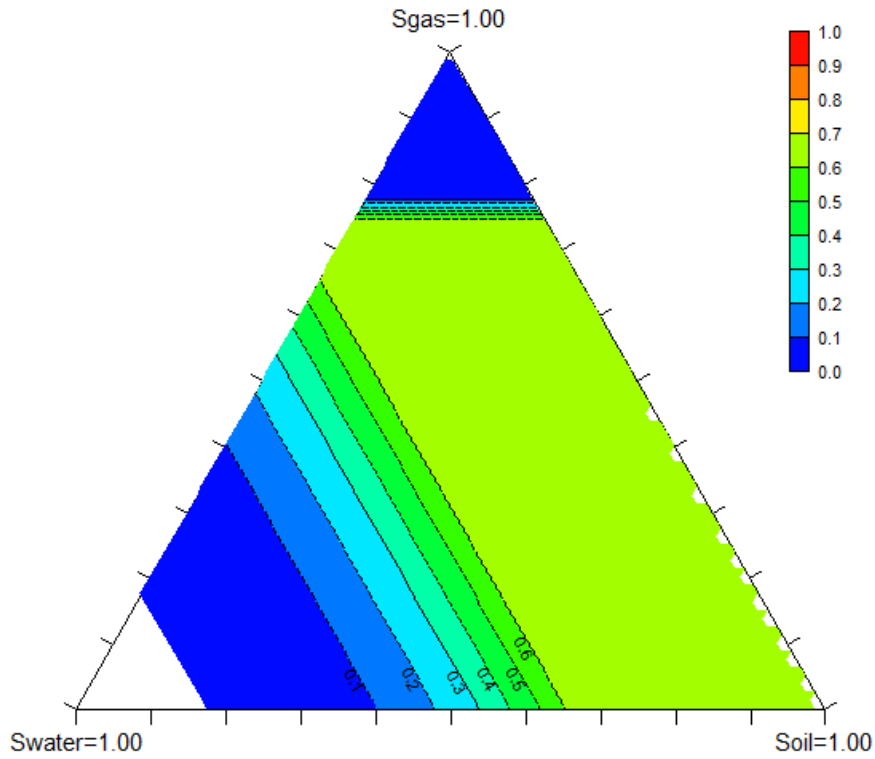


Figure 5.21 Input Ternary Diagram of $k_{r{o}}$ for Liquid and Gas Phase, Matrix

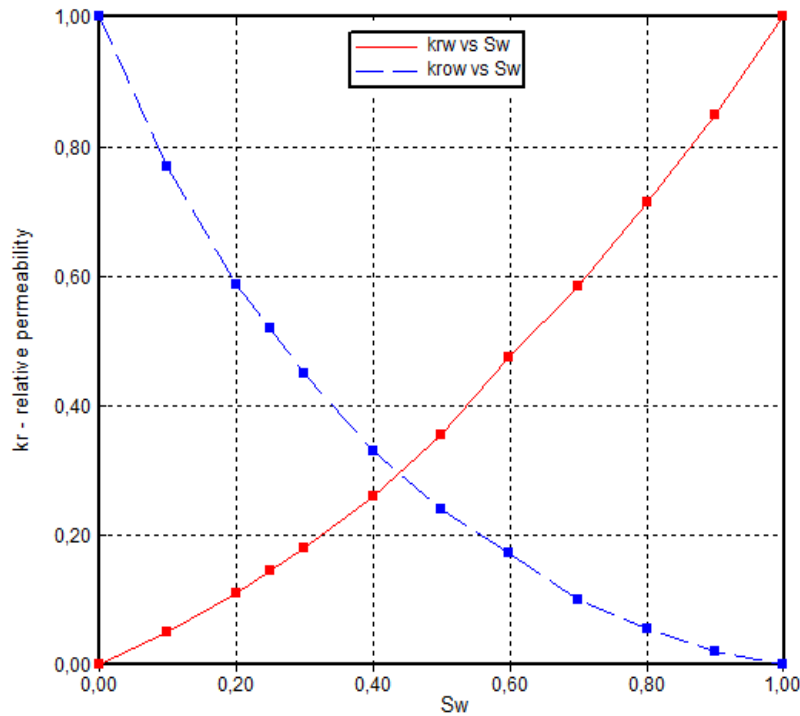


Figure 5.22 Input Oil/Water Relative Permeabilities for Liquid Phase, Fracture

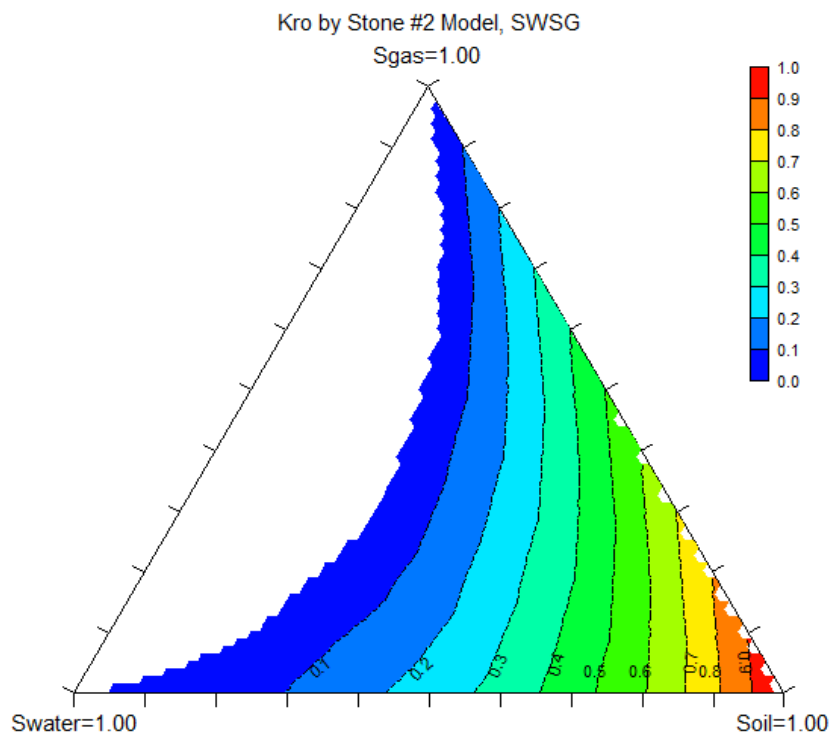


Figure 5.23 Input Ternary Diagram of k_{ro} for Liquid and Gas Phase, Fracture

Combined with fluid data, generated tensors are used in the CMG Stars and models are shown from the Figure 5.24 to 5.27, comparatively with conventional DP model.

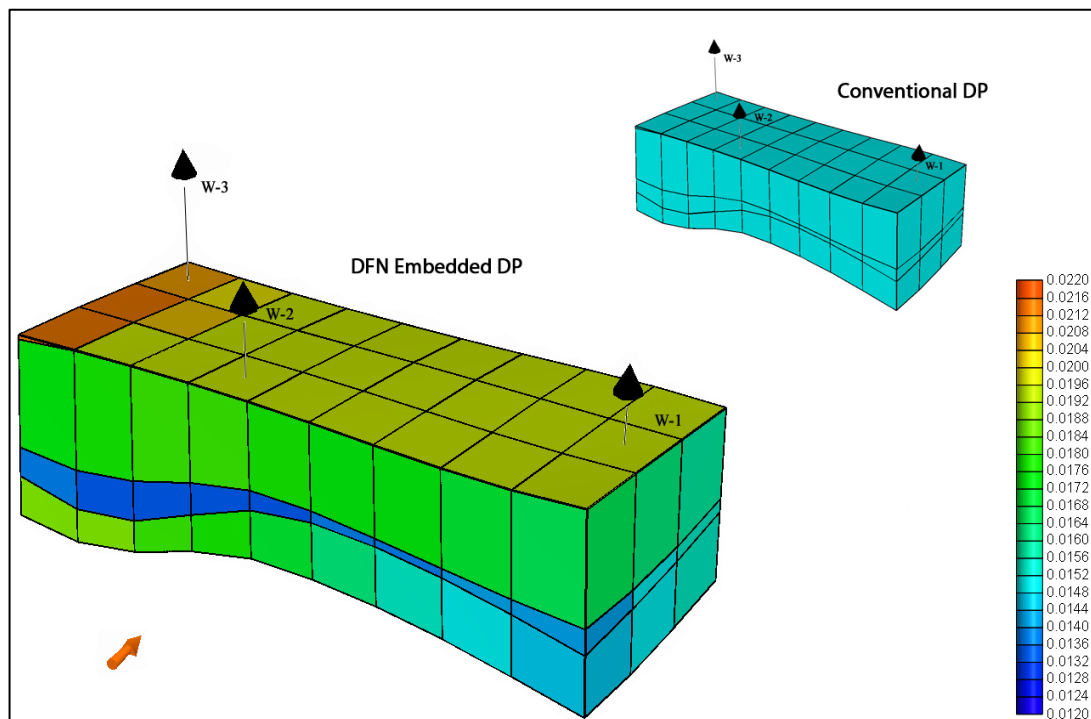


Figure 5.24 DFN Model Generated for Fracture Porosity

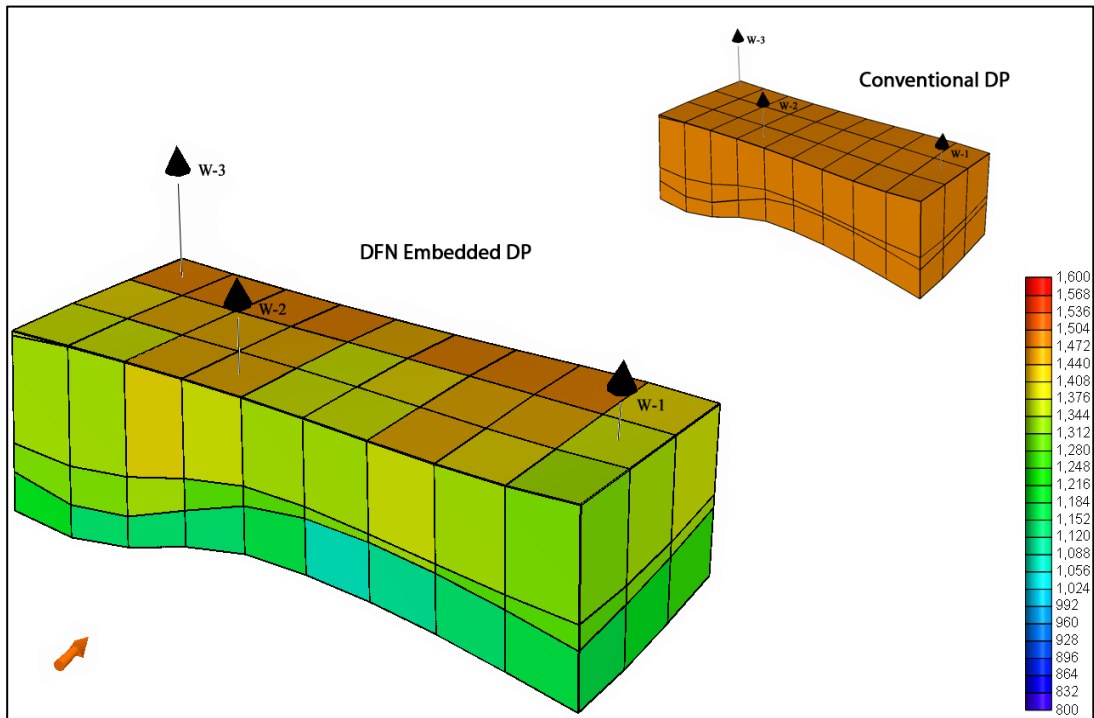


Figure 5.25 DFN Model Generated for Fracture Permeability in x direction

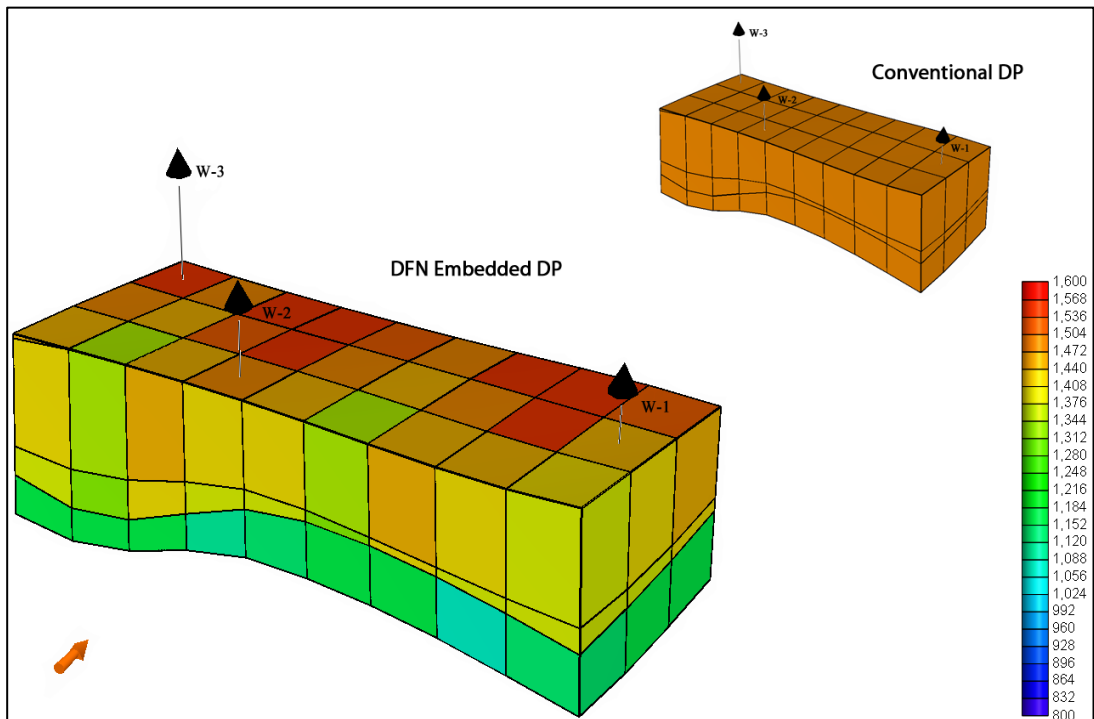


Figure 5.26 DFN Model Generated for Fracture Permeability in y direction

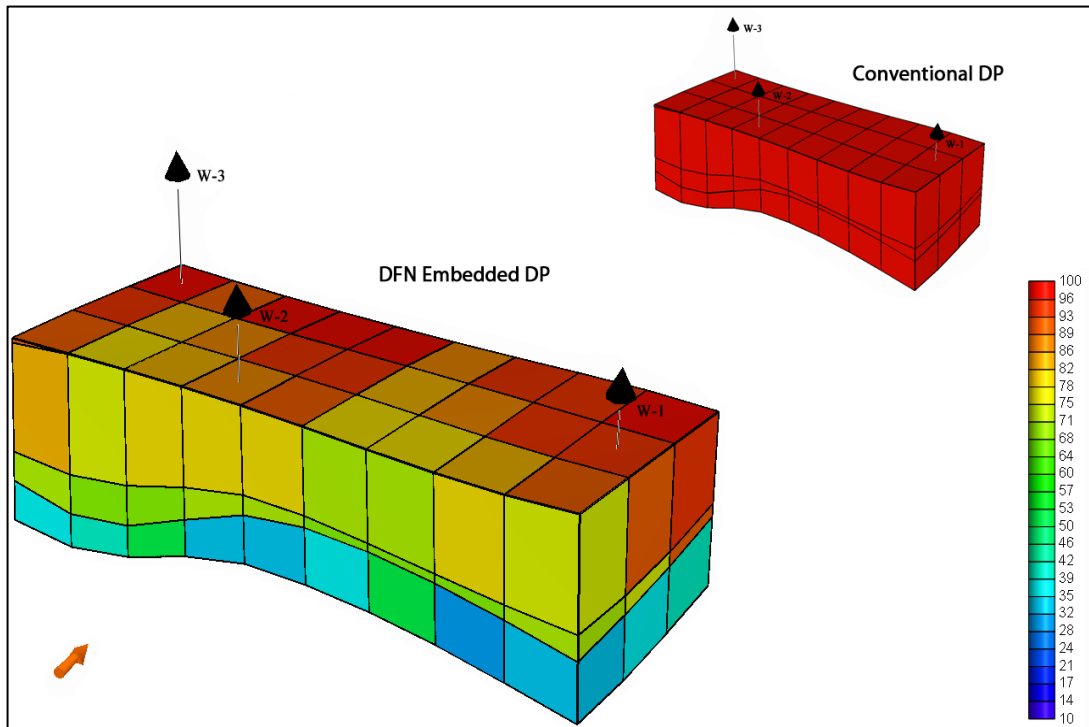


Figure 5.27 DFN Model Generated for Fracture Permeability in z direction

5.5 CMG Stars Output

Finally, DFN embedded DP model is executed and the outputs are demonstrated graphically. Output is compared to conventional model results and field data available; CO₂ injection period is also shown comparatively. Dual-porosity model with constant fracture properties is indicated as a conventional model. Since there are three wells in the sector analyzed, three graphs of oil rates and water cut percentages are shown. In the model, oil rates are imposed to the simulator, therefore, matches obtained in the oil rates shows that prepared model works properly, Figure 5.28, 5.29 and 5.30.

As it can be seen from the Figures 5.29 and 5.30 there is an increase in oil rates after 1986. This year is the start of the CO₂ injection in the field. Well-2 and Well-3 of the analyzed sector are affected from the overall reservoir performance increase after the CO₂ injection has started.

Efficiency comparisons are made on the basis of water cut percentage graphs. Zero values of water cut from the field are not real and shows lack of data during that periods.

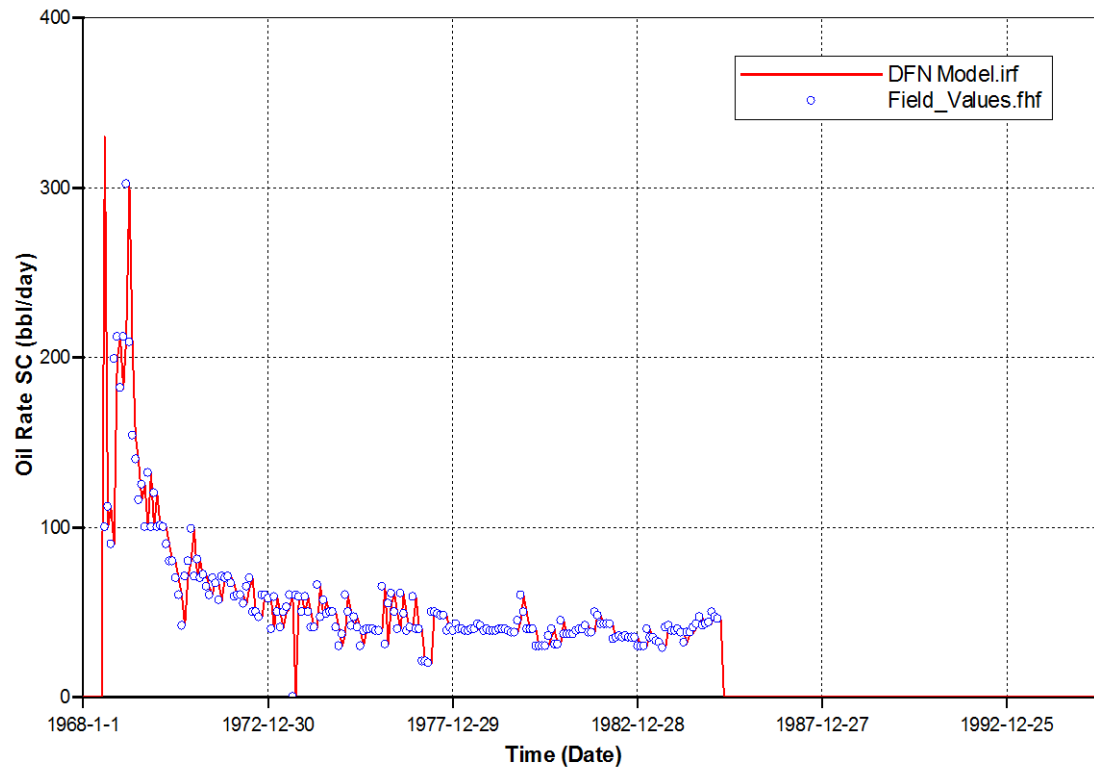


Figure 5.28 Oil Rate Match for Well-1

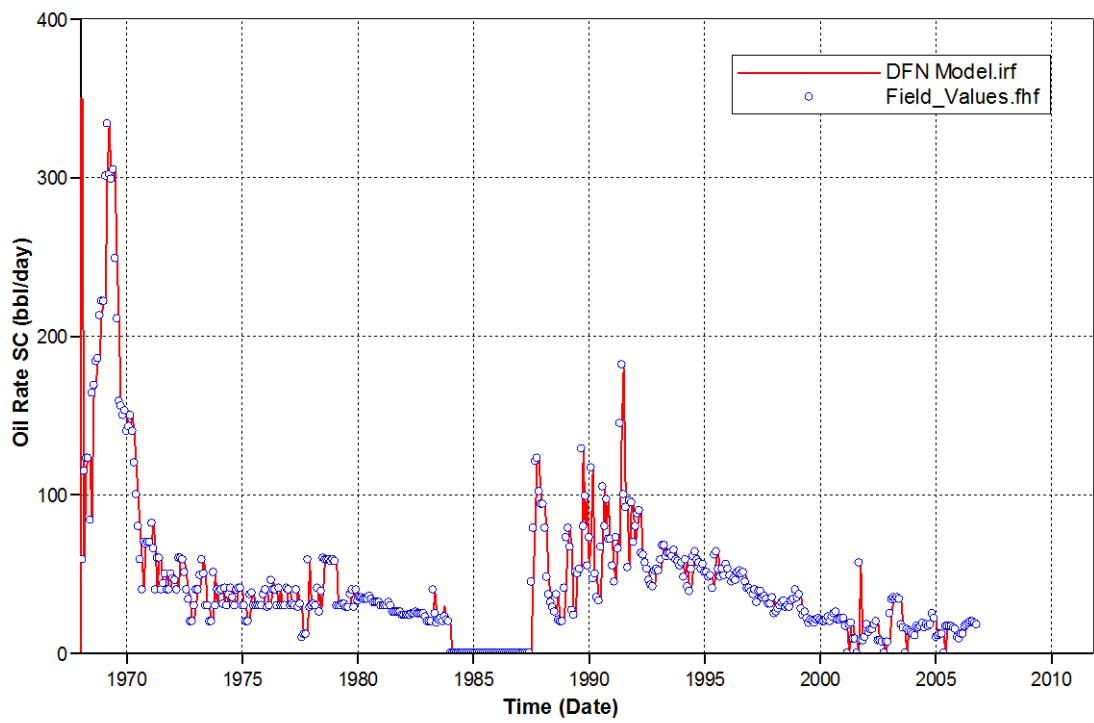


Figure 5.29 Oil Rate Match for Well-2

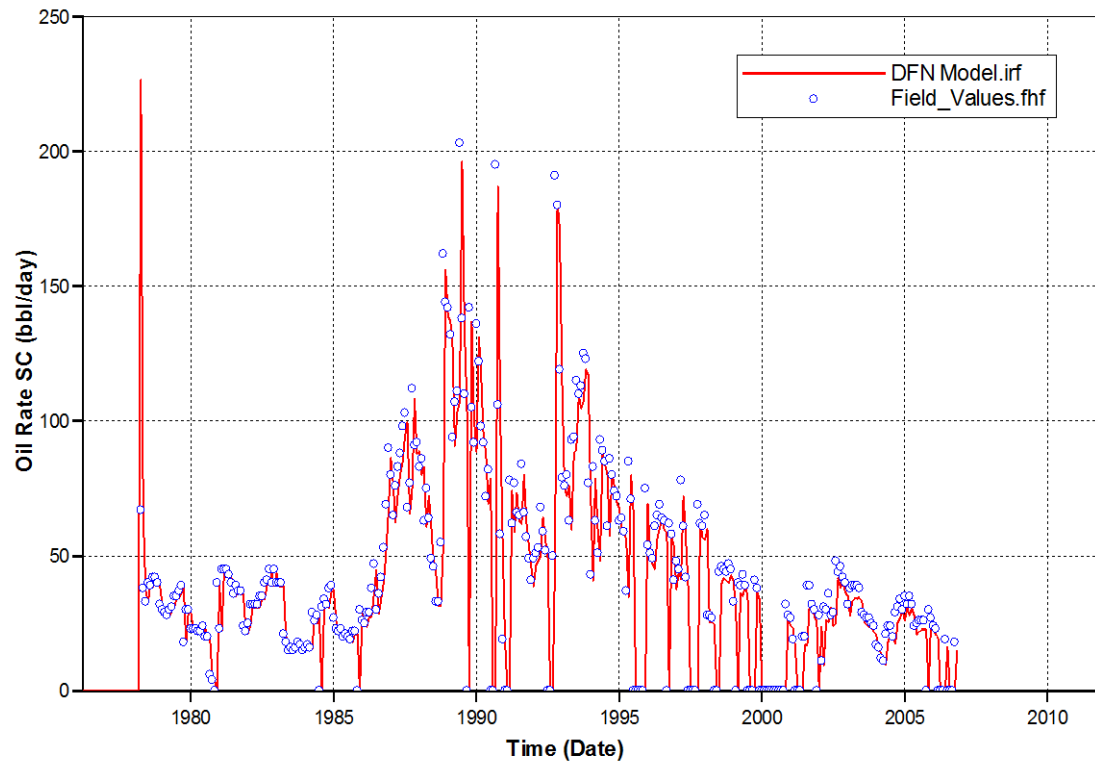


Figure 5.30 Oil Rate Match for Well-3

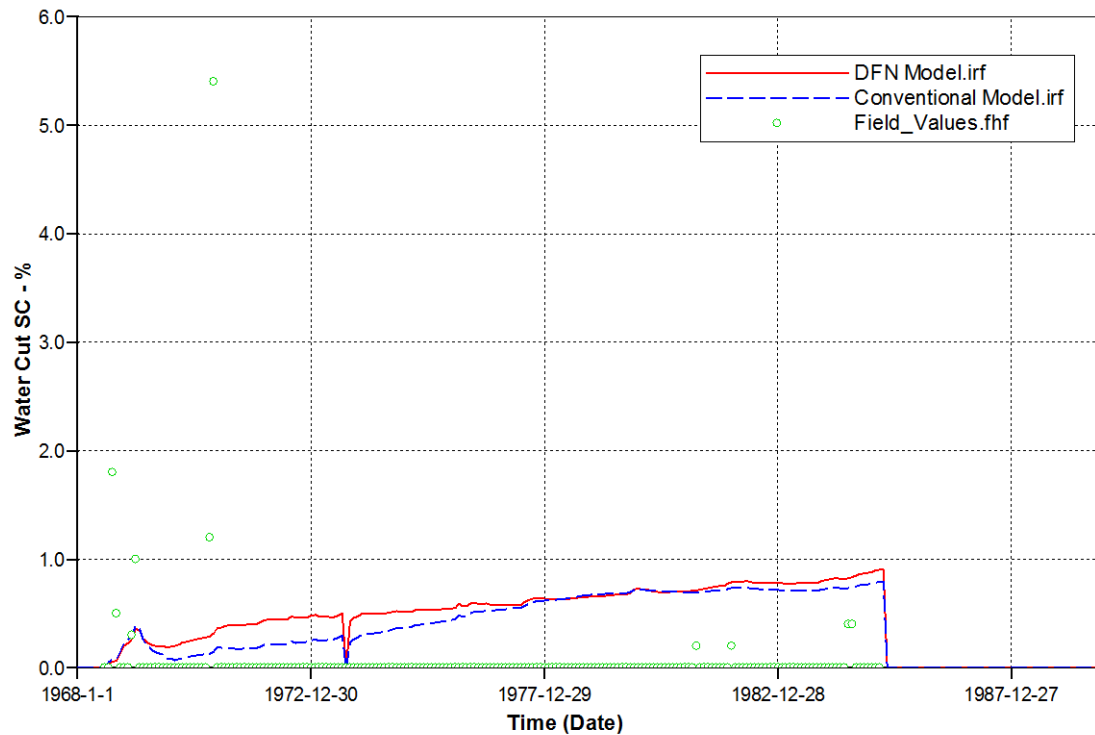


Figure 5.31 Water Cut Matches for the DFN and Conventional Models, Well-1

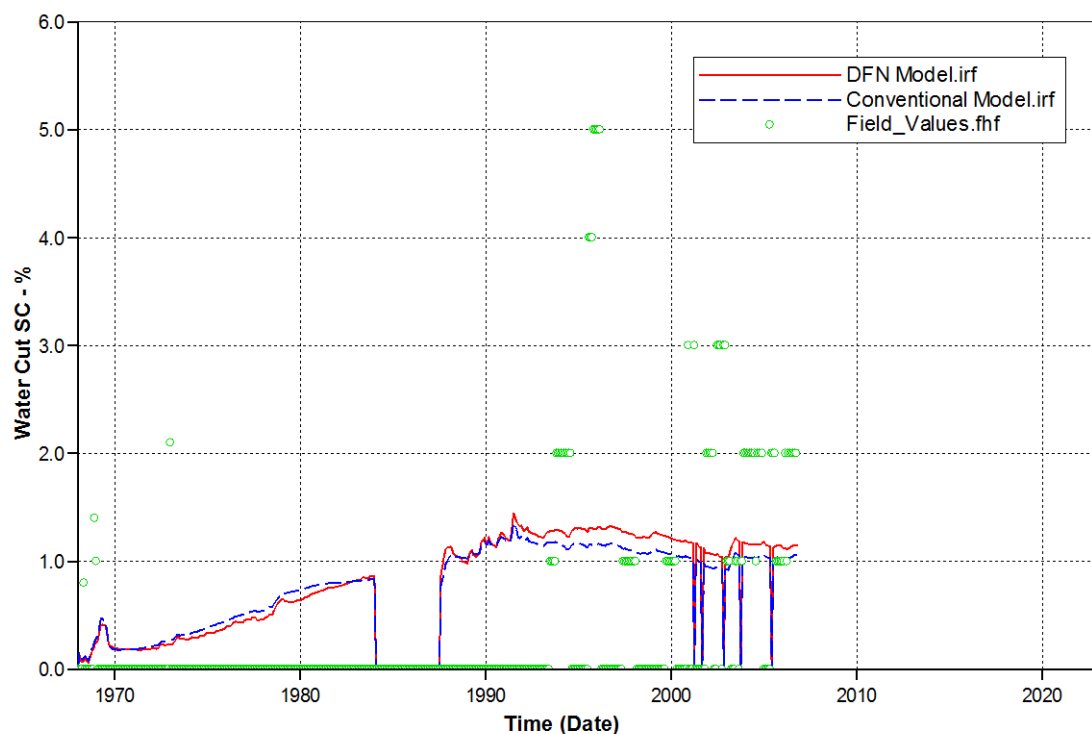


Figure 5.32 Water Cut Matches for the DFN and Conventional Models, Well-2

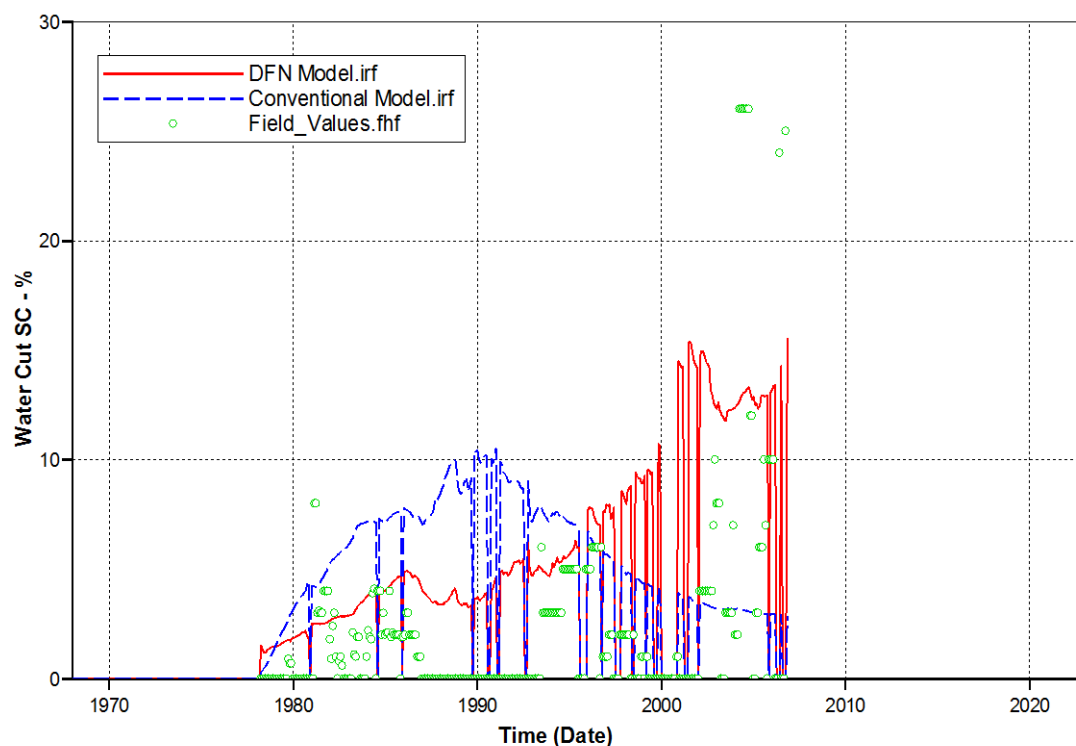


Figure 5.33 Water Cut Matches for the DFN and Conventional Models, Well-3

In the Figure 5.31 water cut comparison for Well-1 is shown. Quantity of the water cut percentage data is not much. Moreover, there is no continuous drastic change in the original field data to understand whether models would be able to catch it. Only slight deviation of DFN output from the conventional model response can be recognized.

Water cut comparison for Well-2 is shown on the Figure 5.32. Again quantity of water cut percentage values is not big and only slight deviation in the correlation can be seen between DFN and conventional model.

Much better results derived for the Well-3 and it can be seen on the Figure 5.33. In this case, even with the naked eyes DFN shows much better estimates with the highest number of water cut value among all three wells. Conventional model lacks to estimate hump in the last period and DFN is much better for predicting this increase in water cut even though there is a decrease in oil rate in the same period as it can be seen from the Figure 5.30.

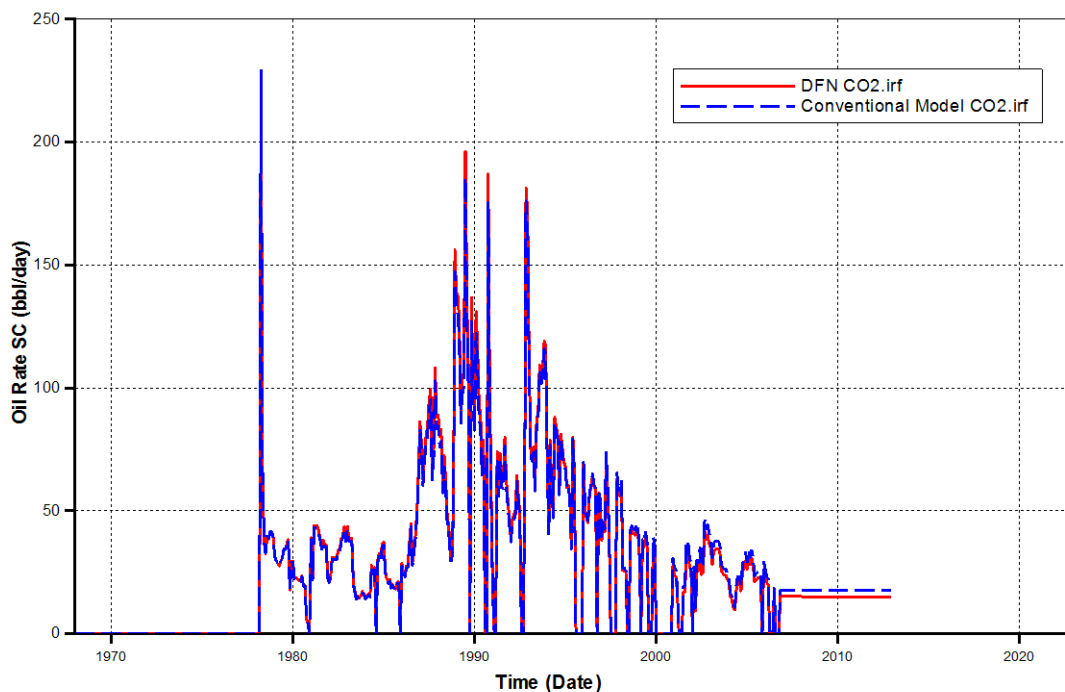


Figure 5.34 Oil Rate Extrapolation in DFN and Conventional Models, Well-3

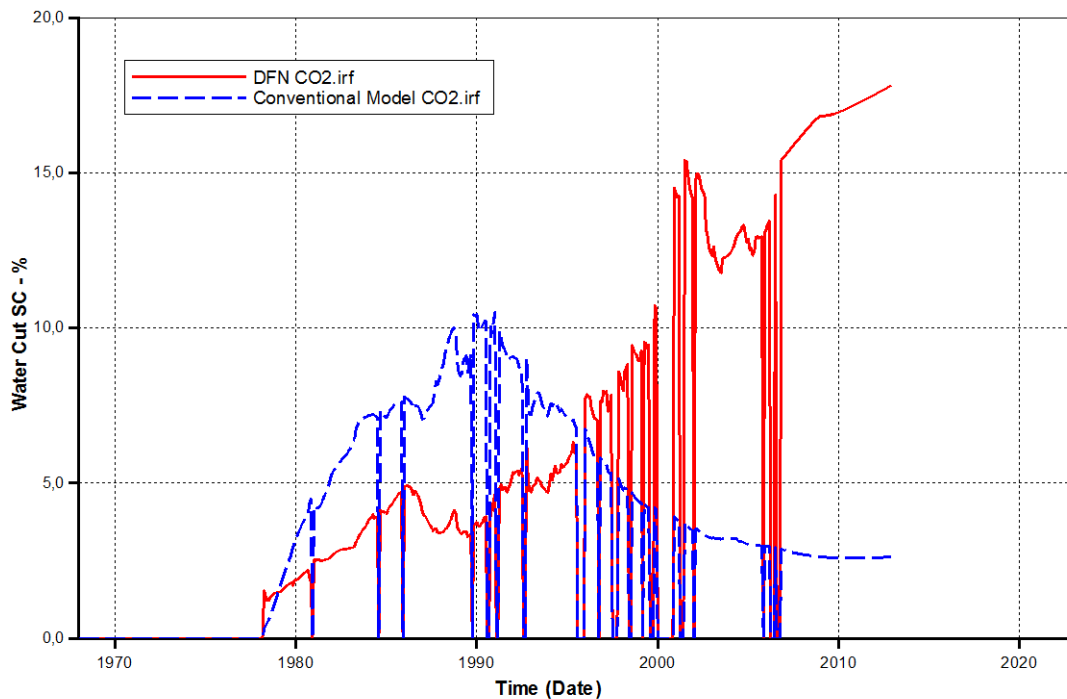


Figure 5.35 Water Cut Extrapolation in DFN and Conventional Models, Well-3

Finally, CO_2 with the 150 °F temperature and 1800 psi surface pressure is injected from the Well-1 and Well-2 starting from the last day of the available field production data, till the end of November, 2012 with the 10^6 scf/day injection rates. Forecasted production from Well-3 demonstrated graphically in a comparative manner. As expected, conventional model results for oil and water production shows deviation with DFN model approach. Although oil rate difference is as much as three or four bbl per day, water cut shows fifteen percent difference. Oil rate extrapolation for these two models is shown in the Figure 5.34 and water cut in the Figure 5.35.

CO_2 is injected from the second and third layers of reservoir and gas mole fractions for both conventional and DFN models on the last day of injection is shown from the Figure 5.36 to 5.39. Conventional model shows the circular decrease of CO_2 mole fraction starting from well side because of constant fracture properties, however, this is not the same for DFN model. Fracture orientation, density and aperture affect the flow direction and decrease rates, therefore, produced mole fraction figures are much heterogeneous than the results of conventional model.

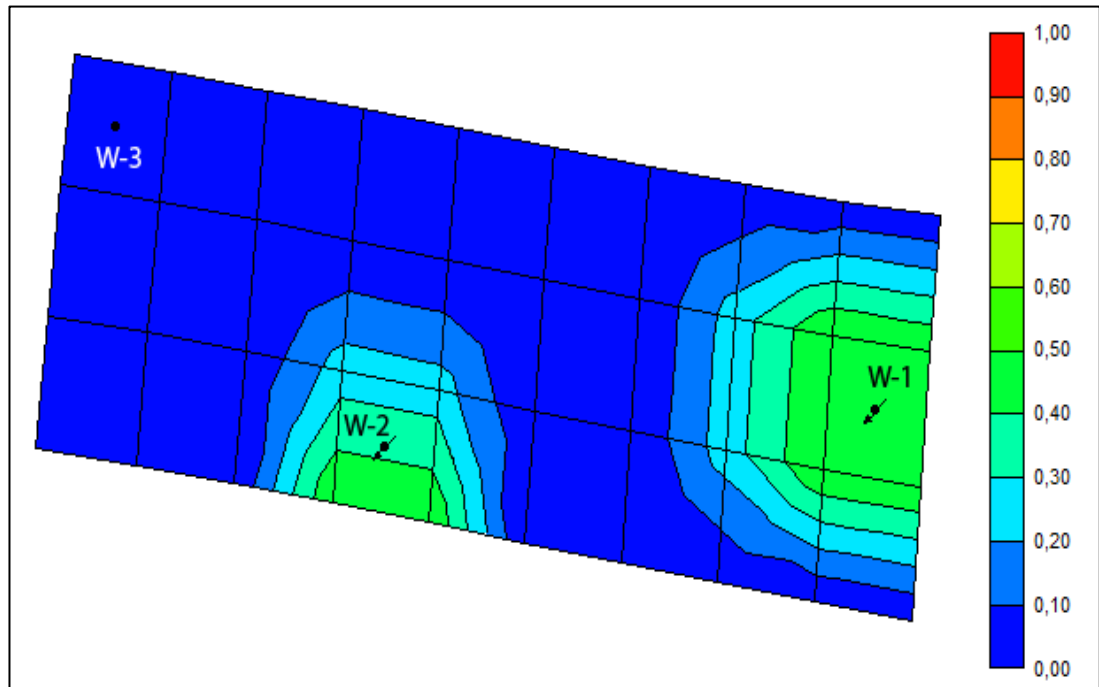


Figure 5.36 Conventional Model, CO₂ mole fraction at the end date, Layer 2

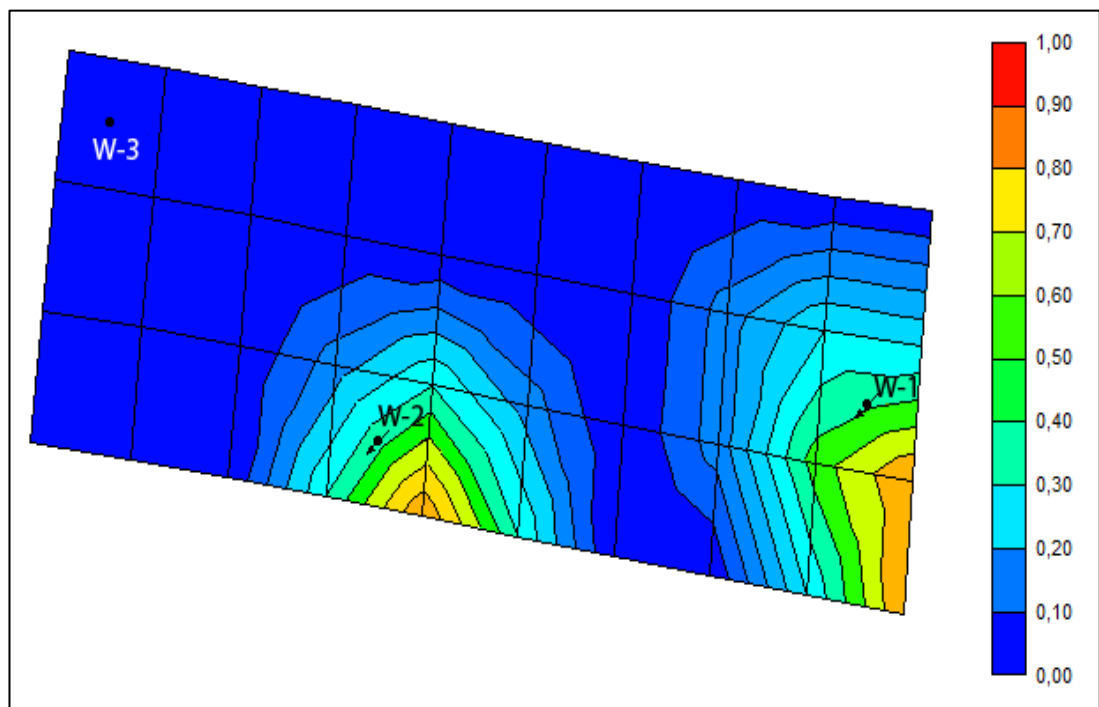


Figure 5.37 DFN Model, CO₂ mole fraction at the end date, Layer 2

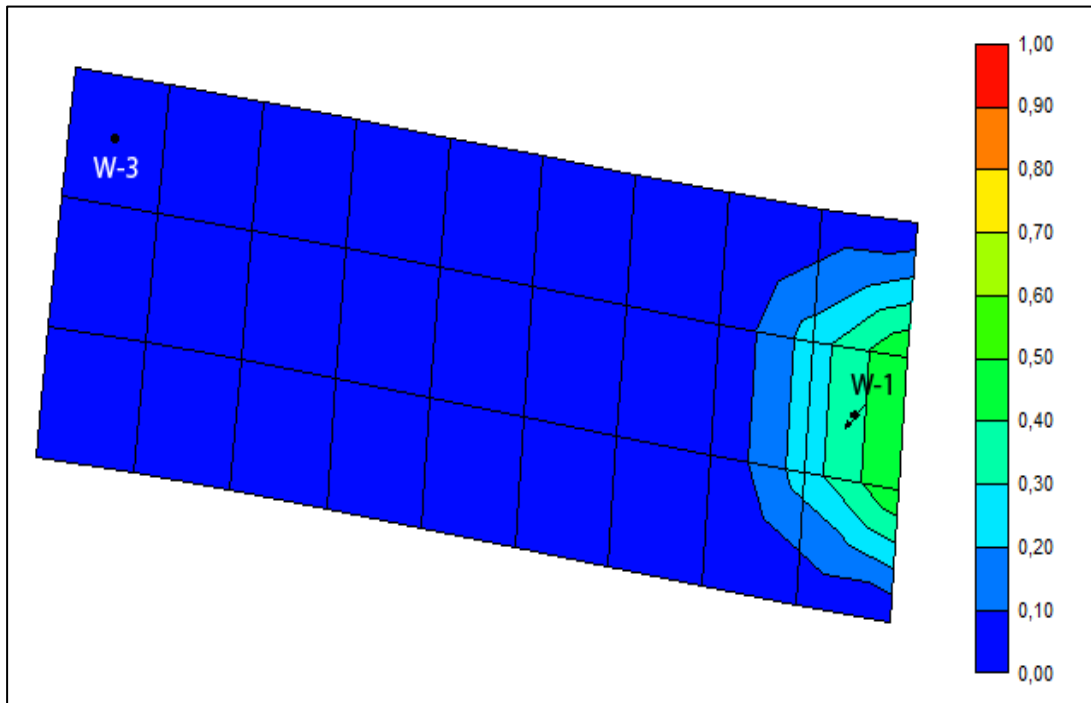


Figure 5.38 Conventional Model, CO₂ mole fraction at the end date, Layer 3

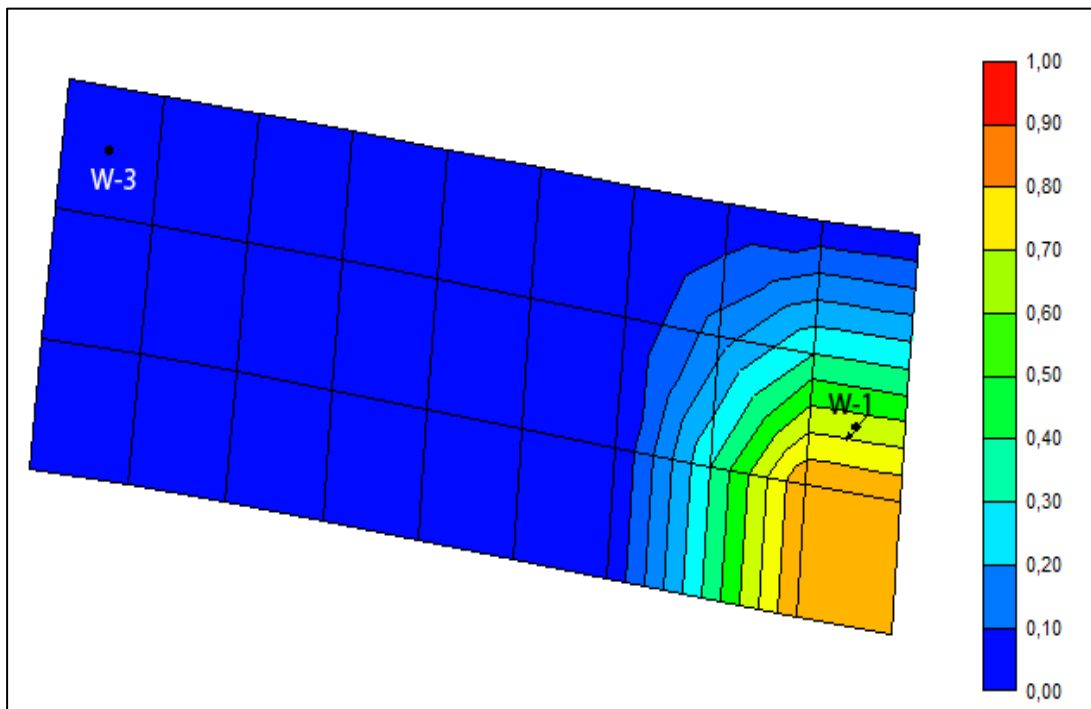


Figure 5.39 DFN Model, CO₂ mole fraction at the end date, Layer 3

CHAPTER 6

CONCLUSION AND RECOMMENDATION

In overall, this study approves what it is stated in the literature. With the help of DFN models, reservoir fractures are better characterized, hence better production estimates can be derived whenever qualified data is available or in other words, data quality is as much important. However, in the case field studied core analysis for the Well-1 and Well-2 is lacking and quality of well test analysis is low for these two wells.

As it mentioned in Chapter 3, core scanner analyses derived from core samples belonged to the Well-3. Aperture distribution and the other parameters derived from core samples are used for all sector area, although it belonged to the well mentioned. After the results of the simulation, it can be concluded that fracture shows much heterogeneity than assumed, even to the wells close to the Well-3. To obtain better results for the Well-1 and Well-2, core samples from these wells need to be gathered and analyzed.

Well test matches obtained while dynamic analysis are also indicative of better fracture characterization around Well-3. No fracture information from Well-1 and Well-2 make DFN less effective for these wells. Consecutively, relatively poor matches both in well test simulations and production history are obtained for these two wells. Therefore, several actions can be taken for better fracture modeling which clarified below.

Enhancing information about fractures or other porosity systems such as vugs, wormhole channels; increasing quality of the data; changing model approaches can be the possible ways to get the better results. As it is mentioned in Section 2.5 adding storage capacity of the vugs, modeling wormhole channels as pipe elements may increase effectiveness and is necessary for carbonate reservoirs. Moreover, connectivity study can be carried out for these wells which may increase model realism. Static method for the connectivity measurement can be done by percolation while dynamic method is capacitance model. Lastly, since, there is no information about fractures around the Well-1 and Well-2 those parts of the reservoir sector can be modeled with EPM while using DFN approach around Well-3.

Finally, good matches obtained in Well-3 while usage of DFN makes the results of this approach while CO₂ injection more reliable than the results of conventional model approach. It indicates less oil production and higher water cuts which can affect reservoir development scenario.

REFERENCES

- Adler, P. M., and Thovert, J. F., “Fractures and fracture networks”, Kluwer Academic Publishers, Dordrecht, 1999
- Akin, S., Celebioglu, D., and Kalfa U., “Optimum Tertiary Steam-Injection Strategies for Oil-Wet Fractured Carbonates” SPE 120168 presented at the 2009 SPE Western Regional Meeting, San Jose, California, USA, 24-26 March
- Akin, S., Petroleum Reservoir Characterization Lecture Notes, Revised ed., Petroleum and Natural Gas Engineering Department, METU, Ankara, 2008
- Arslan, I., Akin, S., Karakece, Y., and Korucu, O., “Is Bati Raman Heavy Oil Field a Triple Porosity System?” SPE 111146 presented at the 2007 SPE/EAGE Reservoir Characterization and Simulation Conference, Abu Dhabi, UAE, 28–31 October
- Bairos, K. P., “Insights from use of a 3D Discrete-Fracture Network Numerical Model for Hydraulic Test Analysis”, M.S. Thesis, The University of Guelph, Ontario, Canada, 2012
- Balzarini, M., Nicula, S., Mattiello, D., and Aliverti, E., “Quantification and description of fracture network by MRI image analysis”, Magnetic Resonance Imaging, Elsevier, 2001, 539–541
- Bear, J., Dynamics of fluids in porous media, American Elsevier, New York, 1972
- Berkowitz, B., “Characterizing flow and transport in fractured geological media: A review”, Advances in Water Resources, Elsevier, August-December 2002, 861-884

Bertsekas, D. P., and Tsitsiklis, J. N., Introduction to Probability, 1st ed., Athena Scientific, Belmont, Massachusetts, 2002

Bogatkov, D., “Integrated Modeling of Fracture Network System of the Midale Field”, M.S. Thesis, University of Alberta, Canada, 2008

Dershowitz, W.S., and Doe, T.W., “Practical applications of discrete fracture approaches in hydrology, mining, and petroleum extraction” Proceedings of International Conference on Fluid Flow in Fractured Rocks, Atlanta, 1988, 381-396

Dershowitz, W.S., Doe, T.W., Uchida, M., and Hermanson, J., “Correlations between fracture size, transmissivity, and aperture” In Culligan et al., Soil Rock America, Proceedings of the 12th Pan-American Conference on Soil Mechanics and Geotechnical Engineering, 2003, 887-891

Dershowitz, W. S., Einstein, H.H., “Characterizing rock joint geometry with joint system models” Rock Mechanics and Rock Engineering, January-March, 1988, 21-51

Dershowitz, W. S., and Pointe, P. R., “Discrete Fracture Network Modeling for Carbonate Rock”, Golder Associates Inc., 2007, 153-157

Dershowitz, W. S., Pointe, P. R., and Doe, T. W., “Advances in Discrete Fracture Network Modeling”, Proceedings of the 2004 US EPA/NGWA Fractured Rock Conference, Portland

Doe, T., and Geier, J., Interpretations of Fracture System Geometry Using Well Test Data, SKB Stripa Project TR 91-03, Svensk Kärnbränslehantering AB, 1990

El-Bassiounya, A. H., and Jones, M. C., “A bivariate F distribution with marginals on arbitrary numerator and denominator degrees of freedom, and related bivariate beta and t distributions”, King Saud University, Saudi Arabia and The Open University, UK, 2008

Erlich, E., "Relative Permeability Characteristics of Vugular Cores", Paper SPE 3553 Presented at the 1971 Fall Meeting of SPE, New Orleans, Louisiana, October 3-6

FracMan User's Manual Release 7.2, Golder Associates Inc., 2009

Fransson, A., "Literature survey: Relations between stress change, deformation and transmissivity for fractures and deformation zones based on in situ investigations", Chalmers University of Technology and Swedish Nuclear Fuel and Waste Management Co., Stockholm, 2009

Gilman, J. R., "Practical Aspects of Simulation of Fractured Reservoirs", International Forum on Reservoir Simulation 2003, Baden-Baden, Germany, 23-27 June

Horne, R. N., Modern Well Test Analysis: A Computer-Aided Approach, 4th ed., Petroway Inc., USA, 1990

Jambayev, A. S., "Discrete Fracture Network Modeling for a Carbonate Reservoir", M.S. Thesis, Colorado School of Mines, Golden, Colorado, 2013

Jin, G., and Pashin, J. C., "DFNModeler: An Efficient Discrete Fracture Network Modeler", International Coalbed Methane Symposium 2007, Alabama, Tuscaloosa, Paper 0709

Kantar, K., Karaoguz, D., Issever, K., and Varana, L., "Design Concepts of a Heavy-Oil Recovery Process by an Immiscible CO₂ Application", SPE11475 JPT, February, 1985, 275-283

Keller, A. A., "High Resolution CAT Imaging of Fractures in Consolidated Materials", Elsevier Science Ltd., April-June, 1997, 155.e1-155.e16

Kume, A., Walker, S. G., "On the Fisher-Bingham distribution", Institute of Mathematics, Statistics and Actuarial Science, University of Kent Canterbury, UK, 2009

Lanru, J., and Stephansson, O., Fundamentals of Discrete Element Methods for Rock Engineering: Theory and Applications, 1st ed., Elsevier, Amsterdam, 2007

Lee, C. C., Lee, C. H., Yeh, H. F., and Lin, H. I., "Modeling spatial fracture intensity as a control on flow in fractured rock", Environ Earth Sci., Department of Resources Engineering, National Cheng Kung University, Taiwan, 2010

Lee, J., Choi, S., and Cho, W., "A Comparative Study of Dual-Porosity Model and Discrete Fracture Network Model", KSCE Journal of Civil Engineering, vol. 3, No. 2, 1999, 171-180

Lemos, J., "A distinct element model for dynamic analysis of jointed rock with application to dam foundation and fault motion", PhD Thesis, University of Minnesota, USA, 1988

Long, J. C. S., Gilmour, P., and Witherspoon, P. A., "A model for steady fluid flow in random three dimensional networks of disc-shaped fractures", Water Resources Research, August, 1985, 1105-1115

Long, J. C. S., Remer, J. S., Wilson, C. R., and Witherspoon, P.A., "Porous media equivalents For networks of discontinuous fractures" Water Resources Research, June, 1982, 645-658

Milton, U. S., and Arnold, J. C., Introduction to Probability and Statistics, Principles and Applications for Engineering and Computing Sciences, 3rd ed., McGraw-Hill Inc., New York, 1995

Mohammad, K. F., "Flow modeling in fractured reservoirs", Stanford University, California, USA, 2002

Nelson, R. A., Geologic Analysis of Naturally Fractured Reservoirs, 2nd ed., Gulf Professional Publishing, Houston, 2001

Ohen, H. A., Enwere P., Daltaban S., "The Role of Core Analysis Data in the Systematic and Detailed Modeling of Fracture Carbonate Reservoir Petrophysical

Properties to Reduce Uncertainty in Reservoir Simulation” paper SCA2002-49,
Society of Core Analysts Annual Meeting, Monterey, CA, USA, 2002

Pruess, K., and Narasimhan, T. N., “A practical method for modeling fluid and heat flow in fractured porous media”, Society of Petroleum Engineers Journal 25, February, 1985, 14-26

Reddy, J. N., An Introduction to the Finite Element Method, 3rd ed., McGraw-Hill Inc., New York, 2006

Snow, D. T., “A Parallel Plate Model of Fractured Permeable Media”, PhD Thesis, University of California, Berkeley, USA, 1965

Spivak, A., Karaoguz, D., Issever, K., and Nolen, J. S., “Simulation of Immiscible CO₂ Injection in a Fractured Carbonate Reservoir, Bati Raman Field, Turkey” SPE 18765 presented at the 1989 SPE California Regional Meeting, California, 5-7 April

STARS User’s Guide, Computing Modelling Group Ltd., 2004

Van Golf-Racht, T. D., Fundamentals of Fractured Reservoir Engineering, 2nd ed., Elsevier Science Publishing Company Inc., New York, 1982

Warren, J. E., and Root, P. J., “The behavior of naturally fractured reservoirs”, Society of Petroleum Engineers Journal, September 1963, 245-255